

Progress of nanoscience in China

Yu-Liang Zhao^{1,4}, Yan-Lin Song², Wei-Guo Song², Wei Liang⁵, Xing-Yu Jiang¹, Zhi-Yong Tang¹,
Hong-Xing Xu³, Zhi-Xiang Wei¹, Yun-Qi Liu², Ming-Hua Liu², Lei Jiang^{2,1,6}, Xin-He Bao⁷,
Li-Jun Wan², Chun-Li Bai^{8,†}

¹National Center for Nanoscience and Nanotechnology, Beijing 100190, China

²Institute of Chemistry, Chinese Academy of Sciences, Beijing 100190, China

³Institute of Physics, Chinese Academy of Sciences, Beijing 100190, China

⁴Institute of High Energy Physics, Chinese Academy of Sciences, Beijing 100049, China

⁵Institute of Biophysics, Chinese Academy of Sciences, Beijing 100190, China

⁶School of Chemistry and Environment, Beijing University of Aeronautics and Astronautics, Beijing 100191, China

⁷Shenyang Branch, Chinese Academy of Sciences, Shenyang 110004, China

⁸Chinese Academy of Sciences, Beijing 100864, China

Corresponding author. E-mail: †clbai@cashq.ac.cn

Received March 10, 2013; accepted April 1, 2013

Fast evolving nanosciences and nanotechnology in China has made it one of the front countries of nanotechnology development. In this review, we summarize some most recent progresses in nanoscience research and nanotechnology development in China. The topics we selected in this article include nano-fabrication, nanocatalysis, bioinspired nanotechnology, green printing nanotechnology, nanoplasmonics, nanomedicine, nanomaterials and their applications, energy and environmental nanotechnology, nano EHS (nanosafety), etc. Most of them have great potentials in applications or application-related key issues in future.

Keywords nanoscience, nanotechnology, nanomaterials, nanomedicine, plasmonics, fabrication, catalysis, nano EHS (nanosafety)

PACS numbers 81.07.-b, 73.63.-b, 78.67.-n, 87.85.-d, 81.16.-c, 81.05.U-

Contents			
1	Introduction	257	
2	Recent research progress in China	258	
2.1	The controllable fabrication	258	
2.2	Nano catalysis: From vision to reality	259	
2.3	Bio-inspired nanotechnology	262	
2.4	Green printing nanotechnology	263	
2.5	Nano plasmonics	265	
2.6	Nanomedicine	267	
2.6.1	Novel therapeutics of cancer with nanomedicine	267	
2.6.2	Micelles-based drug delivery system	268	
2.7	Nanomaterials and their applications	269	
2.7.1	Molecular nanomagnets	269	
2.7.2	Carbon-based nanomaterials	270	
2.7.3	Rare earth nanomaterials and fabrication	274	
			276
			277
			278
			279
3	Perspectives	280	
	References		281

1 Introduction

China is one of the pioneering countries that initiated nanoscience and nanotechnology research. Through more than 20 years' investments and projects implementation, Chinese nanoscientists are active in exploring nanoscale sciences in multidisciplinary fields, and have made a number of breakthroughs in the studies on various fields of emerging fundamental researches and nanotechnology applications [1].

In this review, we summarize some most recent progresses in nanoscience research and nanotechnology development in China, mostly in recent five years. We mainly focus on the topics below including nanofabrication, nano catalysis, bioinspired nanotechnology, green printing nanotechnology, nano plasmonics, nanomedicine, nanomaterials and their applications, such as carbon-based materials, rare earth nanomaterials and fabrication, energy nanomaterials, environmental nanomaterials, nanotechnology for analytical sciences, nano EHS (nanosafety), and other emerging fundamental researches and nanotechnology applications. For example, Chinese scientists have discovered useful methods for the controllable fabrication of nanomolecules (Section 2.1), and controlled synthesis of CNTs and the directed assembly of metal and metal oxide NPs within the CNTs for nano catalysis, and found an unique confinement effect within CNTs, which modulates the redox properties of catalyst NPs to turn the vision of molecule-level catalyst design into reality (Section 2.2). Bio-inspired nanotechnology is one of the featured researches in China. During more than 15 years, we have created a bio-inspired research direction, from simply mimicking natural structures randomly to designing and programming ideal structures, from neglecting function and seeking unique function to exploring natural functional system and to integrating various nanomaterials to artificial functional system (Section 2.3). Green printing nanotechnology developed by Chinese chemists is a green plate-making printing technology which abandons the idea of photosensitizing, with advantages of low cost, almost no pollution, convenient and fast (Section 2.4). Nano plasmonics aims at light manipulation at nanometer scale and has large application potentials in many fields, including information technology and sensing. Researchers in China have achieved considerable progresses in this field, including a cutting edge progress in shell-isolated nanoparticle-enhanced Raman spectroscopy (SHINERS) (Section 2.5). In nanomedicine field, rather than using nanoparticles as carrier of delivering traditional drugs by other scientists worldwide Chinese scientists opened a completely new way of using low-toxic nanoparticles directly as the cancer therapeutic agents, without carrying any traditional drugs. This way has been demonstrated to be more effective. These established a new concept in drug designs (Section 2.6). Nanomaterial science is one of the most developed fields in China, in particular, molecular nanomagnets, controllable synthesis of carbon-based nanomaterials, inorganic nanomaterials (Section 2.7). China is one of the biggest countries of rare earth (RE) resources and production in the world. So, the RE nanomaterial research is an

other featured area in China. Because of the sharp fluorescent emission *via* intra- $4f$ or $4f-5d$ transitions with abundant f -orbital, configurations show unique features including narrow emission band widths (<10 nm), long luminescence lifetime (μs – ms range) and low long-term toxicity (Section 2.7). Synthesis and properties investigation of Non-IPR fullerenes have attracted much attention from the community. Moreover, nanotechnologies for energy conversion and storage (Section 2.7), environmental nanomaterials (Section 2.7), nanotechnology for analytical sciences (Section 2.8), and nano EHS (Section 2.9), etc., are also the most active areas in China.

It is noted that many other significant progresses have been made by Chinese scientists. We have no space to mention all of them here in one article. We speculate that the reader may find some of them in other articles of this special issue.

2 Recent research progress in China

2.1 The controllable fabrication

The controllable fabrication of self-organized molecular adlayers on solid substrates is an important step towards integration of functional molecules into molecular devices. Li-Jun Wan *et al.* at Institute of Chemistry, Chinese Academy of Sciences (ICCAS) developed the sub-molecular resolution scanning tunneling microscopy (STM) in various chemical environments to probe the structures of molecular architectures at nanoscales. The self-assemblies of calixarene, metallo-supramolecular compounds, organic semiconductors and the structural transition of supramolecular assembly under external stimuli have been revealed [2, 3]. Understanding of the driving forces behind the formation of molecular nanoarchitecture through self-assembly process enables the rational design of nano-patterned, hierarchical molecular assemblies. For example, by simply tuning the attached alkyl chains attached to aromatic core, the target graphene-like molecules can be organized into different nano-patterns (Fig. 1) [4]. Furthermore, modular bottom-up design principle has been developed to fabricate sophisticated supramolecular architectures [5]. It has been shown that the molecules can self-assemble into nanoporous networks on surface with periodically arranged voids, which can serve as template to accommodate guest molecules with desired functions. Furthermore, the flexible template has been designed to be tunable according to the size, functional groups, and aggregation state of guest molecules. On the other hand, host-guest interaction can also be utilized

to extend the nanostructure in direction vertical to the substrate, resulting in the ordered molecular nanojunction array. The surface “host-guest” assembly further enriches the concept of supramolecular chemistry and is a promising strategy to design the molecular nanostructures. The well-controlled molecular nanostructures on surfaces provide interesting platform to understand fundamental physical chemistry, such as surface chirality, molecular electrochemistry, and new approach to construct molecular electronic device unit [6]. For example, by inducing topochemical polymerization on the well-organized monomers on surface, the highly ordered molecular nanowires with semiconductor property can be fabricated.

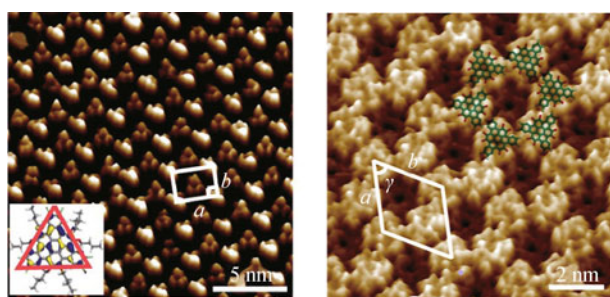


Fig. 1 Structural evolution of the self-assembly of a graphene molecule on HOPG from an alternate “up-down” structure to honeycomb structure upon changing the attached alkyl chain length.

Li-Jun Wan *et al.* have also been devoted to designing and fabricating nanostructures and nanomaterials for environmental remediation and energy applications based on the comprehensive understanding of self-assembly of molecules and nanometer-sized building blocks. Besides the intensive investigation of a great amount of self-assembled molecular adlayers on solid substrates, they extended their understanding of the interaction and self-assembly of molecules to fabricate three dimensional molecule-based nanomaterials. Kinds of organic molecules with designed functional groups were chosen to effectively fabricate organic nanomaterials and even highly-ordered superstructures via self-assembly techniques. For example, a variety of porphyrin, fullerene, and other organic semiconductor nanorods, nanowires, nanobelts, and nanotubes etc. have been achieved and been demonstrated the potential applications in photoelectronics and sensors [7]. Beyond that, their understanding of self-assembly at molecular level has been applied onto nanometer-sized building blocks (such as nanocrystals, nanorods, etc.) to prepare micro/nanomaterials with desirable structures aiming at practical applications, especially in environmental remediation and energy storage. Several general eco-friendly synthesis routes have been developed to fab-

ricate hierarchically structured metal oxides or sulfides, including iron oxide, cobalt oxide, titanium oxide, alumina, vanadium oxide, copper oxide and ZnS, etc., with two or more levels of structure for combining the advantages from different structural levels [8]. The overall size in micrometer or submicrometer level endues materials with desirable mechanical properties and processibility, such as robustness, facile species transportation, easy recovery, regeneration, etc. The size of building blocks in nanometer level provides a high surface area, a high surface-to-bulk ratio, a high activity and efficient charge carrier transport. In combination of these features, the hierarchically structured materials assembled from nanobuilding blocks exhibit either excellent adsorption capacities for toxic heavy metal ions in water or high photocatalytic degradation activities for efficient removal of organic pollutants in water. Some of the products, such as iron oxide and alumina nanostructured materials, have been successfully used in pilot apparatus for polluted water treatment and demonstrated their practical applications in low-cost and efficient environmental remediation. On the other hand, the nanomaterials with such structures showed the promising potentials in energy conversion and storage. For example, Pt nanocrystals assembled hollow structures and their composites delivered high activities as efficient electrocatalysts for fuel cells [9]. Vanadium (V) oxide hedgehog-like hierarchical structures, in which nanoparticles interconnect to nanorods and these nanorods circle around to hollow microspheres, showed enhanced electrochemical properties with high capacity and remarkable reversibility when used as cathode materials in lithium-ion batteries [10]. In order to further take benefits of nanosize effects (such as favorable Li storage kinetics, enhanced structure stability and new Li storage mechanism for higher capacity) and overcome its shortcomings (such as low thermodynamic stability and high surface reactivity), several general strategies in designing efficient electrode materials for lithium-ion batteries have been explored and demonstrated by tremendous work in Li-Jun Wan’s group [11–15]. Self-assembled nano/micro hierarchical structures, hierarchical three-dimensional (3D) interpenetrating mixed conducting networks, issue-oriented nanostructured composite design, and controlled surface coating have been proved as effective ways to construct high-performance electrode materials for energy storage devices (Fig. 2).

2.2 Nanocatalysis: From vision to reality

Since the 20th century, catalysis has been a core technology in the many aspects of national economy, including petroleum refining, fertilizer/chemical synthesis, and

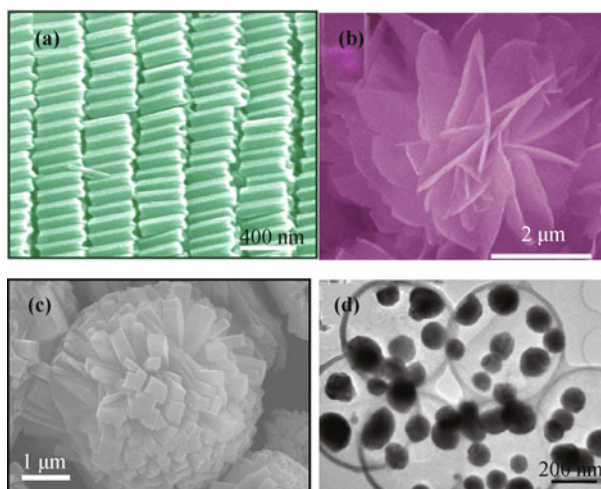


Fig. 2 (a) self-organization of porphyrin hollow hexagonal-nanoprisms; (b) iron oxide microflowers for efficient removal of toxic metal ions in water; (c) hedgehog-like hierarchical nanostructures of V_2O_5 ; and (d) Sn-nanoparticles encapsulated elastic hollow carbon spheres for high-performance electrode material in lithium-ion batteries.

pollution control. Tailoring catalysts or catalytic processes at the molecular level have long been the “Holy Grail” of catalytic chemistry, or even the field of chemistry. It is now known that key elementary steps of surface catalytic reactions, such as the adsorption of reactants, the diffusion of intermediates and the desorption of products, all involve electron transfers between the catalyst surface and the reactive species. In another words, the electronic structure of catalyst surfaces directly influences the activation barrier (i.e., reactivity) and reaction channels (i.e., selectivity) of a catalytic process. The development of nanoscience and nanotechnology has thus brought a huge opportunity for catalysis researchers to tailor the electronic structures of catalysts and subsequently, the catalytic processes.

Confinement effect in carbon nanotubes: Xin-He Bao *et al.* at Dalian Institute of Chemical Physics (DICP) have developed techniques to assemble catalytically active components inside the CNT channels [16–18]. The technique involves the cleaning of freshly prepared CNTs, chemically tailoring CNTs to the desired sizes, and filling CNTs with catalytically active NPs. More specifically, one could first deposit metal NPs (such as silver, iron, etc.) onto the outer surface of CNTs, which could introduce defects on CNTs through catalytic oxidation. CNTs were then leached by nitric acid, cutting CNTs of micron-scale length into the fragments of 100–500 nm in length. Shortened CNTs help the filling of catalyst NPs, which was also facilitated by chemical functionalization and ultrasonic treatments. Consequently, metal or metal oxide NPs could be uniformly dispersed

inside the CNT channels with high efficiency ($> 85\%$). The size of NPs could be controlled within the range of 2 to 5 nms.

The confinement effect of CNTs on catalyst NPs could significantly enhance their catalytic performance in hydrogenation/dehydrogenation reactions. For instance, iron NPs confined in MWCNTs (Fe-in) were investigated for the Fischer–Tropsch synthesis (FTS) reaction, a key reaction to convert syngas into liquid fuels. Compared with iron catalysts dispersed on the outer wall of MWCNTs (Fe-out), Fe-in forms more easily the highly active iron carbide species during the reaction. The catalytic yield of higher hydrocarbons (C_{5+}) from Fe-in is approximately twice the yield (Fig. 3) from Fe-out [19–21].

Adopting the same principle, the researchers assembled Rh–Mn NPs into CNTs, which were subsequently used for the synthesis of ethanol from syngas. As expected, the electron-deficient character of the CNT cavity alters the reduction performance of catalyst NPs, facilitating the adsorption and dissociation of CO and the formation of C2 oxygenates, mainly ethanol. The ethanol yield from Rh–Mn NPs inside the CNTs is significantly higher than that from Rh–Mn NPs outside the CNTs [22] (Fig. 3). Overall, the above results suggest that the unique catalytic properties of CNT-confined nanocatalysts originate from the “synergetic confinement effect”, characteristic of the CNT-metal composite nanosystem. Combining first-principles calculations and Monte Carlo simulation, Xin-He Bao *et al.* showed that both CO and H_2 molecules are enriched inside the CNT channels owing to the special electronic structure of CNTs. Furthermore, CO was more enriched than H_2 due to the stronger interaction between CO and the interior surface of CNTs, resulting in a higher CO/ H_2 ratio than in the bulk syngas feed. The different distribution of reactant molecules from inside and outside the CNTs could substantially enhance the chemical reactivity and selectivity.

Confinement effect at the metal-oxide interface: Taking advantage of the interfacial confinement effect, i.e., the strong interaction between ferrous centers and the precious metal surface, Xin-He Bao *et al.* designed and synthesized a nanocatalyst system with stable surface coordinatively unsaturated ferrous (CUF) centers. The synergy between interfacial confined CUF centers and the metal support demonstrates a unique catalytic activity at low temperatures for the preferential oxidation of carbon monoxide (PROX) [23, 24]. Under the realistic working conditions of the proton exchange membrane fuel cell (PEMFC), i.e., low temperature and in the presence of water vapor and CO_2 , they can successfully remove trace CO from the hydrogen feed.

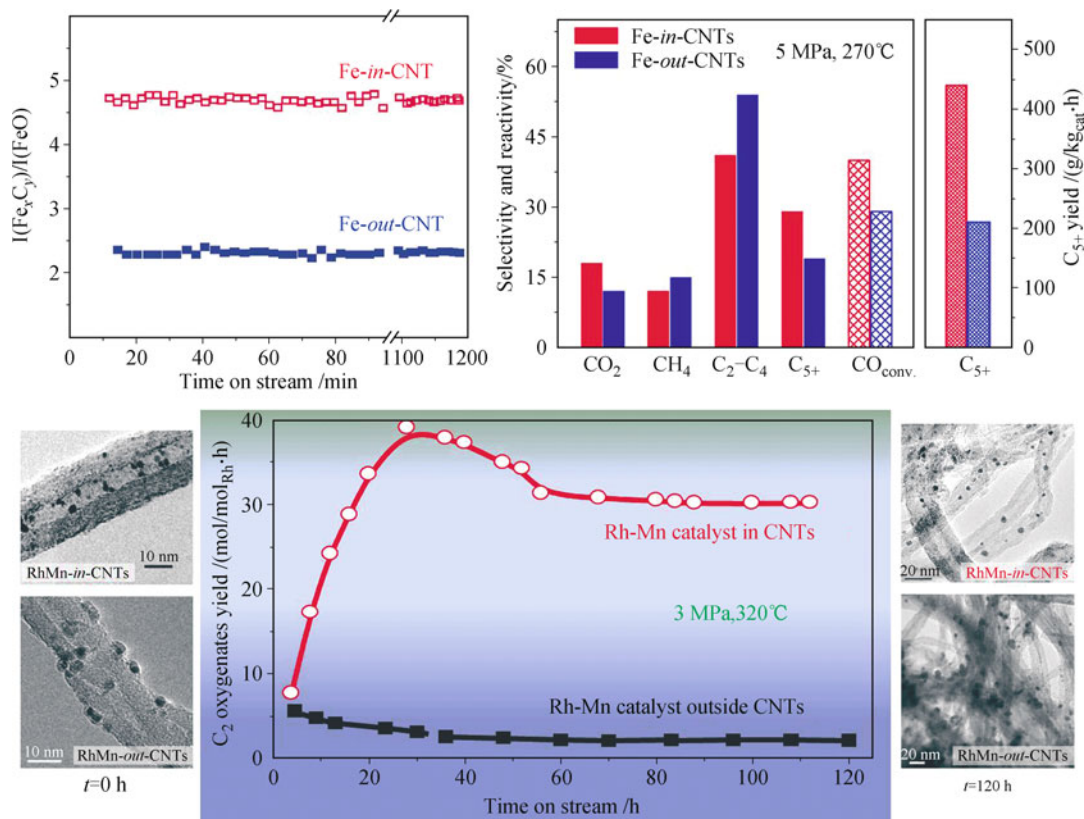


Fig. 3 CNT-confined Fe NPs for the FTS reaction (*upper panel*) and CNT-confined Rh-Mn NPs for the synthesis of ethanol from syngas (*lower panel*).

Selective oxidation is a chemical process involving a wide class of catalytic reactions. When O_2 from the air is used as the oxidant, the reaction often requires a relatively high temperature to dissociate the stable O_2 molecule into the highly active atomic oxygen species, which, on the other hand, exhibit poor selectivity under high temperature conditions, and lead to deep oxidation and the release of large amount of byproducts. Therefore, the design of catalyst to effectively activate O_2 under mild conditions remains a major challenge in catalysis. Inspired by the working principles of dioxygenase, the researchers have used a variety of advanced surface science methods together with theoretical methods, to construct ferrous oxide nanostructures stabilized on the Pt surface, which achieved high efficiency towards O_2 activation under ambient conditions and extraordinary catalytic performance in low temperature PROX and in the selective oxidation of methanol.

To translate the concept perceived from fundamental research into real catalytic applications, the researchers at DICP prepared Pt-Fe catalysts of 3–5 nm size loaded on silica for the removal of trace CO from hydrogen feed (PROX). Their results show that when the molar ratio of reactant gases is 1:0.5:98.5 for $\text{CO}:\text{O}_2:\text{H}_2$, the conversion of CO and the selectivity of CO oxidation can

reach 100% at room temperature, i.e., in the presence of excess hydrogen, atomic oxygen species react selectively with CO to form CO_2 , but not with H_2 to generate water (Fig. 4). In contrast, supported Pt catalysts can achieve only $\sim 5\%$ CO conversion under similar conditions. The active structure of supported Pt-Fe catalysts was characterized by in-situ X-ray absorption near edge structure (XANES), showing the presence of low valent ferrous species during the steady state reaction. When tested under the working conditions of PEMFC, typically at

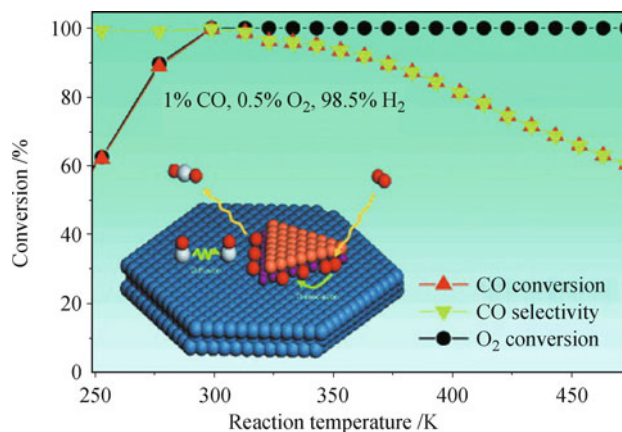


Fig. 4 The catalytic activities of Pt-Fe catalysts supported on silica during PROX reaction.

353 to 373 K and with 25% CO₂ and 20% H₂O in gas, the Pt-Fe catalysts can maintain their excellent performance for more than 1500 hours and yield 92% CO conversion at 353 K.

In the above system, the role of Pt, besides providing adsorption sites for CO, is to interact strongly with surface ferrous centers, enabling an interfacial confinement mechanism approximating the function of protein ligands in an enzyme system. The highly active CUF centers are stabilized by the interface, yet exhibit flexibility to facilitate the reaction cycles. Adopting this concept, one could further explore other substrate materials (e.g., nanostructured carbon materials, composite materials, etc.), which could play a similar role as Pt, but is much cheaper than Pt [25]. Meanwhile, the introduction of interfacial confinement could lead to a better understanding towards the strong metal-support interaction in catalysis and facilitate the design of new highly efficient catalytic systems.

2.3 Bio-inspired nanotechnology

Over millions of years of evolution, nature gestates a huge range of biological materials with amazing functions that serve as a big source of bio-inspiration for functional materials. The integration of bio-inspired study and nanoscience provides an efficient way to prepare nanomaterials with unique properties and develop advanced nanotechnology. In this field the scientists in china have achieved a series of originally innovative and high-level performances. Here we take four topics as examples, bioinspired interfacial nanomaterials with special wettability, bioinspired nanochannel, bioinspired adhesive nanomaterials, and bioinspired strong films.

To fabricate interfacial materials with special wettability has been one of the hot topics in the field of bio-inspired study and surface science. Whatever the superhydrophobic lotus leaves with self-cleaning effect and spider silk with water collective property, these findings reveal that the nano- and micro- scaled structures have strong influence on the macroscopic wettability of solid surfaces. Lei Jiang *et al.* at the Institute of Chemistry, Chinese Academy of Sciences (ICCAS) have explored special wettability of several natural species, like lotus leaf with superhydrophobicity [26] and butterfly wing with anisotropic wettability which revealed the mechanism of their special wettability. These studies set up the base of how to prepare bioinspired interfacial materials with special wettability. They have successfully prepared a series of superhydrophobic interfacial materials with multiple functions [27]. Further by introducing the concept of binary cooperative effect, they developed

single or multiple stimuli responsive “super switches” between superhydrophobicity and superhydrophilicity [28]. Recently they revealed the underwater superoleophobicity of fish scale [29], which provides a new clue to construct hydrogel-based superoleophobic surface and solve the problem of oil pollution. Very recently, they disclosed the secret that spider silk can directionally collect tiny water droplets from the fog (Fig. 5), originating from special periodic spindle-knots structure [30]. Subsequently inspired by spider silk, they developed the artificial polymer nanofibers with capability of fog collection and realize the large-scale fabrication of those functional nanofibers [31]. This finding will bring new insight in how to overcome the droughty problem in some area.

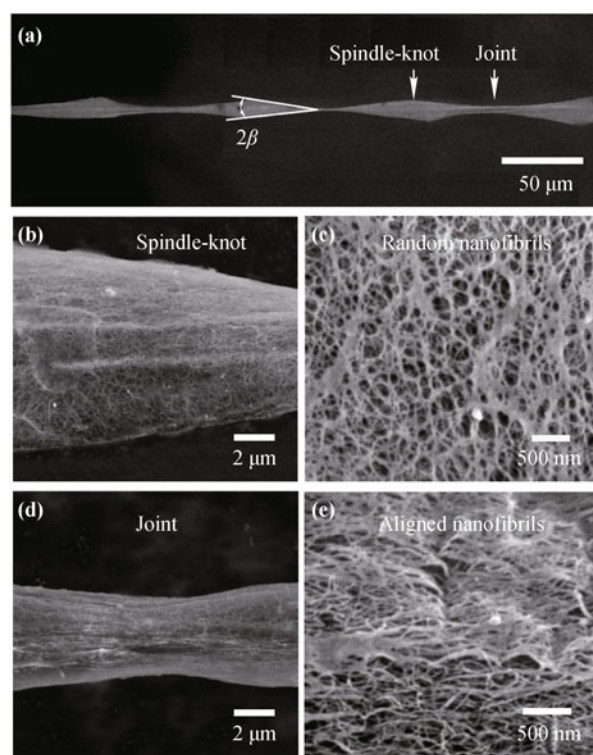


Fig. 5 The special periodic spindle-knots structure of spider silk, which results to directional collection of tiny water droplets from the fog. The spindle-knot is composed by random nanofibrils and the joint is composed by aligned nanofibrils.

Bio-inspired nanochannel is another new branch of bio-inspired study [32]. Cells often use ion channels to communicate chemically and electrically with the extracellular world. Biological ion channels can open and close in response to ambient stimuli for regulating ion permeation through cell membranes. This unique capability is helpful to various important physiological functions in life processes. For example, Lei Jiang *et al.* reported a fully abiotic single-pore nanofluidic energy-harvesting system that efficiently generates electricity by converting Gibbs free energy in the form of a salinity gradient

[33]. The maximum power output with the individual nanopore approaches 26 pW.

The control of adhesive property on a solid surface is very important to fundamental science and practical applications. Most attractively, healthcare-related adhesion between cells and biomaterials or surfaces of biomedical devices remains a great challenge. By mimicking this anisotropic structure, Dong Han *et al.* at National Center for Nanoscience and technology (NCNST) prepared an artificial blood vessel capable to prevent platelets adhering. Another very important progress in adhesive surface is closely related to cancer diagnosis. Traditional immunologists considered that the recognition of cancer cells only depends on molecular recognition. However, in real immune system, microvilli and nanoprotusions of immune cell are usually involved in the recognition process. Shu-Tao Wang *et al.* at ICCAS designed a specific adhesive and high efficient surface to cancer cell by integrating nano-topographic interaction with molecular recognition [34]. This immune-inspired adhesive nanostructured surface can recognize and capture several cancer cells from one billion bloods, which is three order more sensitive than the routine flow cytometry. By further combining with microfluidic, they can achieve about 100% capture of targeted cancer cells [35]. Very recently they fabricated an easy-capture and easy-release surface by introducing exonuclease-cleavable aptamer onto silicon nanowires array [36]. This study broke through the limit of traditional molecular immunology in cell recognition and more importantly it provides a great platform to early cancer detection and therapy monitoring.

Bio-inspired strong films are emerging as one kind of functional nanomaterials derived from the traditional biomineralization fields, which is associated with the assembly of nanoscale building blocks. Inspired by biomineralization phenomena Shu-Hong Yu and his team developed a self-assembly approach at air-water-oil interface to prepare strong inorganic/organic hybrid layered films

[37, 38]. For example, the tensile strength of Cu-NO₃-chitosan hybrid film achieved to 160 MPa [38], which is 8 times as high as that of pure chitosan film and surpasses the natural nacre [38]. In addition, inspired from natural nacre, Lei Jiang and his colleagues prepared a transparent, layered nanocomposite hydrogel from poly(N-isopropylacrylamide) and clay [39]. This hydrogel shows excellent mechanical properties and a hierarchical microstructure. This concept to prepare wet-chemical high-performance materials can be used for wide applications, such as tissue-engineering, sensors, artificial muscles, and underwater antifouling materials.

2.4 Green printing nanotechnology

Currently the mainstream plate-making technology in China is Laser Typesetting, and the widely used plate-making technology worldwide is Computer-To-Plate (CTP). Both technologies are based on the photosensitizing mechanism. Therefore these two technologies inevitably include complex processes like exposing, developing, photographic fixing and processing. All the processes cause problems of high cost, time-consuming and serious environment pollution because the photosensitizing needs washing with chemicals. Currently, chemical effluent discharged annually by the print industry in China reaches hundreds of thousands of tons, which contains hundreds of tons of silver and tens of tons of aluminium. This results in serious resource waste along with terrible environment pollution [40].

Completely different from the above photosensitizing technology, Yan-Lin Song *et al.* at ICCAS invented a green printing plate-making technology via controlling the surface wettability with nanomaterials [41]. Figure 6(a) schematically shows the process of green plate-making technology, where the graphic information is first inputted into the computer and then the printing plates can be directly obtained through inkjet printing. The le-

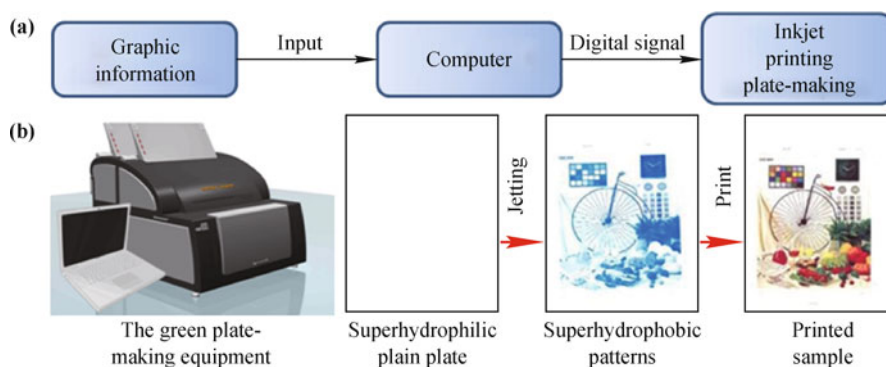


Fig. 6 (a) Scheme of the green plate-making technology; (b) The green plate-making equipment (*left*), and the demonstration of the production process (*right*). It shows that no photosensitizing process is involved in this new technology and the printing plate is directly obtained by inkjetting functional nanomaterials on the nanostructured plate to have the desired superhydrophilic nonimage area and superhydrophobic image area.

ft part of Fig. 6(b) exhibits the green plate-making equipment. The right part of Fig. 6(b) demonstrates the process for the printing plates with the new technology, where the printing plates are directly obtained by inkjetting the functional nanomaterials on the nanostructured plate to have the desired superhydrophilic nonimage area and superhydrophobic image area. No photosensitizing process is involved in this new technology, and the image area and nonimage area are achieved with the strong contrast of the wetting property of the ink on the superhydrophobic and superhydrophilic areas.

It is evident that the green plate-making technology relies on the manipulating of the surface wettability with nanomaterials. Surface wettability is one of the key properties of materials, which is governed by the surface chemistry and topology. In nature, many biological materials exhibit special surface wettability, for example, lotus leaves are superhydrophobic which renders them the property of self-cleaning [42, 43].

Biomimetic research shows that the cooperation of microscale and nanoscale structures as well as the surface chemical composition on these surfaces results in surfaces with tunable wettability [44]. In the case of a droplet sitting on a rough solid surface, Wenzel observed that the apparent contact angle, θ_w , is determined by Eq. (1) [45]:

$$\cos \theta_w = r \cos \theta_Y \quad (1)$$

where r is the surface roughness, and θ_Y is the Young's contact angle, i.e., the contact angle on an ideal flat and homogeneous surface of the same material. From Eq. (1), one can see that a hydrophobic surface ($\theta_Y > 90^\circ$) will be more hydrophobic and a hydrophilic surface ($\theta_Y < 90^\circ$) will be more hydrophilic when the surface roughness is introduced. Cassie and Baxter proposed another model for the droplet sitting on a rough surface with low surface energy, where air is trapped under the droplet [46]:

$$\cos \theta_C = \phi \cos \theta_Y + \phi - 1 \quad (2)$$

where θ_C is the apparent contact angle on the rough surface, θ_Y is the apparent contact angle on the flat surface of the same material and ϕ is the area fraction of the droplet in contact with the solid surface. According to Eq. (2), hydrophobicity can be enhanced by increasing the surface roughness, i.e., decreasing the ϕ .

Both Cassie and Wenzel equations predict that increasing the roughness is the key to having extreme wettabilities, i.e., superhydrophobicity and superhydrophilicity. Yan-Lin Song *et al.* introduced the nanoscale roughness on the plain plate to accomplish the superhydrophilicity. Figure 7 shows scanning electron microscopic (SEM) images of plates fabricated in Yan-Lin Song's group [41]. The roughness can be systematically tuned by controlling the pore size of the plates as demonstrated in the right side of Fig. 7, where the pore size was varied from several tens of nanometers to several hundreds of nanometers. Inset of the left side of Fig. 7 shows that the plate is superhydrophilic.

To achieve the superhydrophobic image area, Yan-Lin Song *et al.* utilized the nanomaterials with low surface energy and different morphologies [47, 48]. The nanomaterials were inkjetted onto the superhydrophilic plate. After drying the nanomaterials clustered on the plate surface with various fractal factors tuned by the morphology of the nanomaterials. Because the nanomaterials were designed to have low surface energy, the area with the nanomaterials is superhydrophobic and oleophilic. As such Yan-Lin Song *et al.* achieved the superhydrophobic image area on the superhydrophilic non-image area on the plate. One has to note that the resolution of superhydrophobic image area can be controlled by manipulating the movement of the three phase contact line of the air/liquid/solid interface. Benefitted from the use of the nanomaterials, the resolution could be as high as submicrometer.

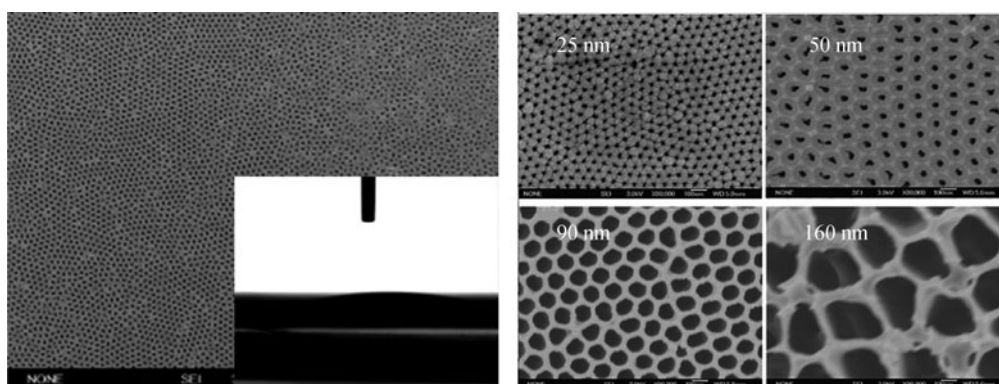


Fig. 7 A scanning electron microscopic (SEM) image of a nanostructured plate (*left*), and the inset shows the complete spreading of water on this plate demonstrating its superhydrophilicity; the right part shows that the pore size on the plate can be tuned by one order of magnitude ranging from tens of nanometers to hundreds of nanometers.

The functional nanomaterials play a key role in this green plate-making technology and some fundamental scientific challenges had to be overcome. On one hand, one has to consider the morphology of jetted nanomaterials, pinning effect of the ink at the border of the image and non-image areas as well as capping agents used for stabilizing the nanomaterials [42]. On the other hand, the rheological and mechanical properties of jetted nanomaterials have to be considered, so that the blocking during the jetting could be prevented and the as-prepared plates have a desired printing durability. Compared with the existing printing technologies, the green plate-making technology has advantages of low cost, almost no pollution, convenient and fast, needless to be in totally dark places. It can be expected that the new technology will substantially reduce the pollution in the print industry.

2.5 Nano plasmonics

Metal nanostructures support surface plasmons (SPs), collective oscillations of free electrons at the metal-dielectric interface, which make the metal structures show many extraordinary optical properties [49]. The studies about SPs have formed an emerging field called “plasmonics” or “nano-plasmonics”. Due to the tight spatial confinement of SPs, light manipulation at nanometer scale becomes possible. Plasmonics is therefore thought as one promising candidate that can scale photonic devices down to the subwavelength scale. One dimensional metal nanostructures, for example, metal nanowires, can support SP propagation over a distance typically ranging from several to hundreds of microns. Metal nanowires, therefore, can be used as optical waveguides like optical fibers, but operate in subwavelength scale. This character makes it attractive to many researchers. For example, Xing Zhu *et al.* at Peking University introduced a bowtie antenna to enhance the coupling of light into the nanowires [50]. Li-Min Tong *et*

al. at Zhejiang University integrated metallic nanowires with semiconductor nanowires and studied the photon-plasmon coupling efficiency [51]. Hong-Xing Xu *et al.* at Institute of Physics, Chinese Academy of Sciences (IOPCAS) have performed a systematic study on the nanowire plasmons. They developed functional elements based on metal nanowire SPs, including router, demultiplexer, modulator and quarter wave-plate [52, 53]. Most strikingly, they demonstrated a complete family of SP-based Boolean logic gates in silver nanowire networks based on coherent interference [54]. By shining light onto the input end of a nanowire, propagating SPs of multiple modes can be launched. SPs of different modes can interfere with each other and generate ‘beating’ patterns along the nanowire which were detected experimentally by using quantum dot imaging technique. In the nanowire network involving two input ends, the phase difference between the two inputs can be manipulated to control the local field distribution. On the other hand, the amplitude of SPs can be tuned by changing the polarization of the incident light. Therefore, by controlling the polarization and the phase of the incident light, a full control over the emissions from the output ends is feasible. By defining the input and output states, a set of Boolean logic operations can be realized, such as AND, OR and NOT. A binary half adder can also be defined in a similar fashion. To demonstrate the potential in optical computing, they went a step further and showed that the SP-based logic gates can be cascaded to carry out more complex operations [55]. In a four-terminal nanowire network, they cascaded the OR and NOT gates and realized a plasmonic NOR gate [Fig. 8(a)]. Although the plasmon-based optical computing is still in its baby age, the revealed potential of developing novel nanophotonic on-chip processor architectures is nevertheless very attractive and deserves further investigations.

Surface plasmons are also involved in many studies of meta materials, a class of man-made materials constructed by precisely shaping and arranging natural ma-

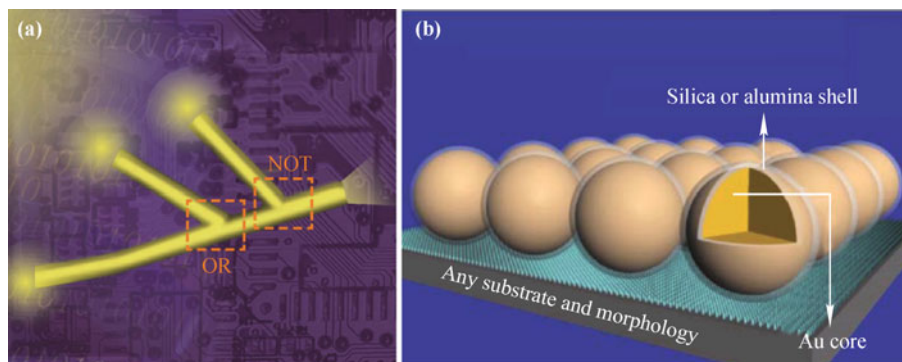


Fig. 8 Schematic drawing of plasmonic NOR gate (a) and SHINERS (b). Reproduced from Refs. [54, 64].

materials, with fantastic applications such as extraordinary optical transmission [56], negative refractive index materials [57] and optical cloaking [58]. Recently, Ru-Wen Peng *et al.* at Nanjing University reported a significant progress on designing transparent metal gratings [59, 60]. Lei Zhou *et al.* at Fudan University made a great progress on converting propagating wave to surface wave with a nearly 100% efficiency by using a special gradient-index meta-surface [61]. Unlike other conversion schemes, the momentum mismatch between the propagating wave and surface wave is compensated by the reflection-phase gradient of the surface. More importantly, the high efficiency conversion can be achieved for any incidence angle larger than a critical value. Therefore, this new idea of gradient-index meta-surface may pave the way for many micro-/nano-optics applications, such as high-efficiency couplers, anti-reflection surfaces and light absorbers.

Many other discoveries on manipulating light propagation are reported. For example, Zhi-Yuan Li *et al.* at IOPCAS drilled a subwavelength hole on a metal film and fabricated grooves of well-designed pattern around it [62]. By shining light onto the structured metal surface, surface plasmons are excited and scattered by the grooves. The interference of the scattered waves results in the reconstruction of the pre-designed image, which can be recorded away from the metal surface in analogy to the conventional holography. Shi-Ning Zhu *et al.* at Nanjing University used a new non-perfectly matched in-plane diffraction method to modulate the SP beam phase and wave front and generated Airy SPs [63]. The unique properties of the SP Airy beam were demonstrated, including non-diffraction, non-dispersion, parabolic focusing and self-healing. Using the same technique, they were able to realize broadband surface plasmon focusing that was further utilized for plasmonic demultiplexer.

Apart from controlling electromagnetic waves for functional devices, the sensing techniques based on SPs are also intensively investigated. SPs in metallic nanostructures are capable to concentrate electromagnetic field into tiny spaces, such as a nanogap between metal nanostructures [64]. The consequence of this unique capability is that a giant electromagnetic field enhancement can be achieved and applied to amplify weak optical processes like the Raman scattering of molecules – a technique known as surface enhanced Raman spectroscopy (SERS). SERS is regarded as an important and promising method to detect a small amount of analytes with high sensitivity. Zhong-Qun Tian *et al.* at Xiamen University have conducted systematic studies on the SERS in transition metal structures [65]. Recently, his group proposed a new approach for SERS, which they called shell-isolated nanoparticle-enhanced Raman spectroscopy (SHINERS)

[Fig. 8(b)] [66]. The idea is to disperse some dielectric-coated gold nanoparticles onto the target samples so that the SERS signals from the molecules sitting below the nanoparticles can be detected. The advantage of SHINERS is that the chemically inert shell prevents the interactions between metal nanoparticles and probed analytes, which may otherwise distort the true Raman spectra. Hong-Xing Xu *et al.* at IOPCAS examined the SERS performances of some novel nanostructures [67–69], and proposed a new excitation configuration for SERS measurements [70]. By using silver nanowire as waveguide, the excitation light is guided to the hot spots several microns away to excite the Raman scattering of the molecules. The remote-excitation makes the illumination at the hot spots confined at nanometer scale, which results in an ultralow background and low damage to the sample. This remote-excitation method provides a new configuration for SERS sensing and may find applications in many new systems.

Similar to the field enhancement effect in particle-particle junctions, SPs can also get localized in a metal tip-film gap. The electromagnetic field enhancement in the gap is experienced by nearby molecules so that the Raman signal of those molecules can be detected. Unlike SERS, tip-enhanced Raman spectroscopy (TERS) can be done in a more controlled way by controlling the tip of the scanning probe microscope. Hong-Xing Xu *et al.* at IOPCAS built a high vacuum TERS system and used it to monitor the chemical reaction processes in situ [71]. The high signal-to-noise ratio TERS spectra they obtained revealed the dimerization process of the probed molecules. The Raman spectra from the new molecules formed in the chemical reaction were misinterpreted by many researchers as originated from the charge transfer between the molecules and the metal. By tuning the laser power, bias voltage or tunneling current, it was demonstrated that the TERS system can control the reaction rate probably due to the hot electrons associated with the localized SPs. This achievement gives insight into the field so-called plasmon-enhanced catalysis, a new-born area that may be promising for the global energy problem. Another recent advance in TERS is measuring single molecule conductance and Raman signal using a “fishing mode” TERS technique, proposed by Bin Ren *et al.* at Xiamen University [72]. They used the TERS technique to monitor the structure of a molecule in the gold tip-film junction at room temperature. This technique allows us to simultaneously obtain the conductance and Raman spectra of single molecule. This is an important progress in understanding the electron transport process in molecular junctions.

2.6 Nanomedicine

2.6.1 Novel strategy for cancer therapy with nanomedicine

Nanostructured materials-based medicines are emerging as robust platforms with immense potentials for effective cancer therapy. However, most current investigated engineered nanoparticles with development for anti-tumor drugs as their goal are under the roof of nanocarriers or drug delivery systems. Yu-Liang Zhao *et al.* at National Center for Nanosciences and Technology (NCNST) & Institute of High Energy Physics, CAS (IHEP, CAS), developed a completely new way in which the hydroxylated metallofullerene $Gd@C_{82}(OH)_{22}$ nanoparticles are directly used as the novel anticancer medicine without upload of any conventional anticancer drugs [73–76]. The metallofullerenol nanoparticle was originally developed for a new generation of high-contrast MRI imaging agent. With nanosurface design [77, 78], Yu-Liang Zhao *et al.* discovered that $Gd@C_{82}(OH)_{22}$ can be an effective and promising anti-tumor agent with much higher inhibitory efficacy of tumor growth versus the current clinical anticancer drugs [69]. More importantly, in contrast to other anticancer agents or nanomaterials, $Gd@C_{82}(OH)_{22}$ nanoparticles do not kill tumor cells (and also normal cells), but rather inhibit tumor growth and metastasis (Fig. 9).

The $Gd@C_{82}(OH)_{22}$ molecule is smaller than 2 nm, but $Gd@C_{82}(OH)_{22}$ tends to aggregate in aqueous solutions and forms dispersed $Gd@C_{82}(OH)_{22}$ nanoparticles with an average diameter of about 100 nm, which

is a ubiquitous property identified in metallofullerenol studies. The nanoparticles at a low dose inhibited hepatocellular damage in association with about 60% inhibition of tumor growth. Although the molar dosage of $Gd@C_{82}(OH)_{22}$ nanoparticles was approximately 1/500 that of the antineoplastic agent cyclophosphamide, their efficiency was much higher under the same experimental conditions, and no observable damage to any important organs [73]. Moreover, $Gd@C_{82}(OH)_{22}$ nanoparticles could reactivate defective endocytosis of cisplatin in cisplatin-resistant (CP-r) cells, and tumor resistance to cisplatin was overcome by treatment with a combination of $Gd@C_{82}(OH)_{22}$ nanoparticles and cisplatin, both *in vitro* and *in vivo* [74]. The high antitumor efficiency of $Gd@C_{82}(OH)_{22}$ nanoparticles is not the result of traditional cytotoxic effects, but rather their direct regulation of the tumor microenvironment. The nanoparticles do not kill tumor cells directly, and less than 0.05% of the exposed dose of $Gd@C_{82}(OH)_{22}$ nanoparticles was distributed in the tumor tissues in tumor-bearing mice [73].

Angiogenesis inhibition is emerging as an important strategy in the development of antitumor therapies. $Gd@C_{82}(OH)_{22}$ nanoparticles represent a new “particulate form” of angiogenesis inhibitor, with more favorable features than the traditional “molecular form” inhibitors. $Gd@C_{82}(OH)_{22}$ nanoparticles have a wide inhibition spectrum of more than 10 angiogenic factors [79]. They largely reduced tumor blood perfusion and efficiently lowered the speed of blood flow to tumor tissues by about 40%. The results of *in vivo* experiments showed that $Gd@C_{82}(OH)_{22}$ nanoparticles potently inhibited

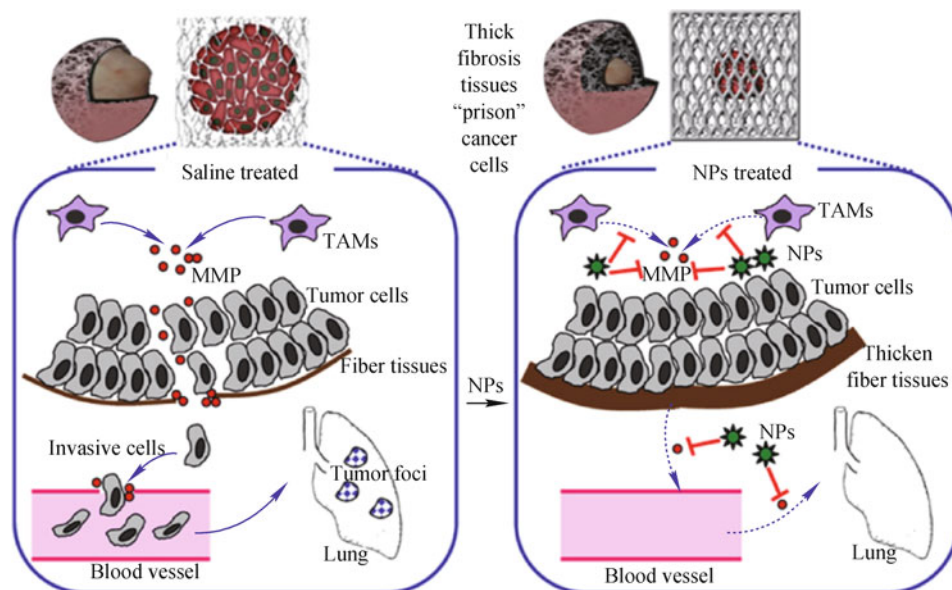


Fig. 9 Schematic representation of possible anti-metastatic mechanism of $Gd@C_{82}(OH)_{22}$ nanoparticles mainly via a MMP-inhibition process. The thick fibrous cage may act as a “prison” to confine invasive cancer cells within the primary site.

tumor growth, with a tumor-inhibition rate higher than the clinical breast-cancer-specific chemotherapeutic agent paclitaxel, at a dosage of Gd@C₈₂(OH)₂₂ nanoparticles one-third the dose of paclitaxel. However, they did not interfere with normal blood vessels, and no changes in the morphology of capillary vessels in normal tissue were seen, including no pronounced abnormalities such as gaps, disfigurements or breaches in the cell layer in blood vessels. These findings confirm the angiogenesis-inhibitory activity of Gd@C₈₂(OH)₂₂ nanoparticles in the tumor microenvironment [79]. Gene expression analysis studies showed that the MMP family was strongly inhibited in response to Gd@C₈₂(OH)₂₂ nanoparticle treatment. The Gd@C₈₂(OH)₂₂ nanoparticles induced dendritic cell maturation and activated Th1 immune responses [80], and potently inhibited the production of MMPs at both the mRNA and protein levels in tumor tissues [81]. Malignant tumors remain an important unresolved medical issue. The tumor microenvironment operates complex mechanisms to become a double-edged sword to either assist tumor cells to become invasive and metastatic or to inhibit their malignant behaviors [82]. To achieve maximal therapeutic efficacy, antitumor agents should not only target tumor cells, but also regulate and normalize the tumor microenvironment to regress tumor progression. Therapeutic agents that target tumor microenvironment thus represent an avenue for the development of novel and effective antitumor therapies. It may become clinically available by using novel nanomedicines.

2.6.2 Poly(ethylene glycol)-phosphoethanolamine micelles-based drug delivery system

As mentioned before, nanoparticles for the drug delivery are another main direction in nanomedicine researches, for example, the polymer-based nanocarriers [83]. Compared with liposomes, polymer-based micelles have many advantages at particle size, stability, drug-loading capacity and releasing kinetics which can be modulated by the structures and physico-chemical properties of the constituent block copolymers. Wei Liang *et al.* have developed one-step self-assembly procedure to encapsulate amphiphilic cationic drugs into PEG2000-DSPE micelles. These micelles have shown better antitumor efficacy than the unencapsulated drugs [84, 85].

For cationic drugs (isoelectric points > 7.4) including doxorubicin hydrochloride (DOX), vinorelbine tartrate (VNR), topotecan hydrochloride (TPT), their encapsulation efficiency are all close to 100%, but anionic gemcitabine hydrochloride (GEM, isoelectric points < 7.4) could not be incorporated [86]. So, that drugs and poly-

mers have opposite charges in solution may be a major factor determining successful encapsulation, and isoelectric points of drugs and polymers may be good parameters to predict the encapsulation efficiency. Drug-loaded micelles were spherical with a diameter between 10 and 20 nm, similar to empty micelles [84–86]. Release profiles of micelles with high drug loading capability were different from that TPT showed obvious initial burst release, while DOX and VNR were slowly released without burst release (submitted). These results prompted us to consider what kind of drugs can be loaded into PEG-PE micelles, how the drugs/polymers interactions and self-assembly process are like. A full understanding of the fate of block copolymer micelle-based drug formulations *in vivo* at the whole body, tissue, and cellular levels has been difficult thus far. For one of the most promising polymers, PEG-PE, used as anticancer drug delivery carrier, providing a greater understanding of their intracellular distribution and cell interactions would help shape the design of highly efficient and less toxic carriers for drug delivery.

They demonstrated that drug loaded PEG-PE micelles maintained intact form before disassembling and releasing their payloads at the cell membrane. Released agents are accelerated to enter cells due to the increased membrane fluidity caused by PEG-PE insertion, which did not affect cell membrane permeability and integrity [87]. Otherwise, PEG-DSPE also enhanced drug uptake by inhibiting p-glycoprotein expression [88]. Encapsulation of drugs in PEG-PE micelles does not change their intracellular distribution but increases their cellular accumulation. For anti-tumor drugs, higher cellular concentration could induce stronger cytotoxicity and more cell apoptosis. *In vivo* investigations reveal that PEG-PE micelles can extravasate from blood vessels to interstitial tissue in an intact form, and can efficiently deliver chemotherapeutic drugs in a higher drug concentrations in circulatory and in lymphatic systems (submitted), maintaining in them a sustained high drug concentration to kill the tumor cells residing there. These investigations provided new insights into the mechanism of polymer micelle delivering drugs into cells, which are helpful for designing a true smart delivery system (Fig. 10).

At present, PGE1-loaded PEG-PE micelles have accomplished phase I clinical trials. Tolerance and pharmacokinetics tests were carried out. From clinical trial results, at the same dose level, PGE1 micelles showed higher plasma concentration compared to alprostadil injection (Kaishi). This study indicated that PGE1 micelles will have superior therapeutic efficacy to Kaishi that are generally used in clinic.

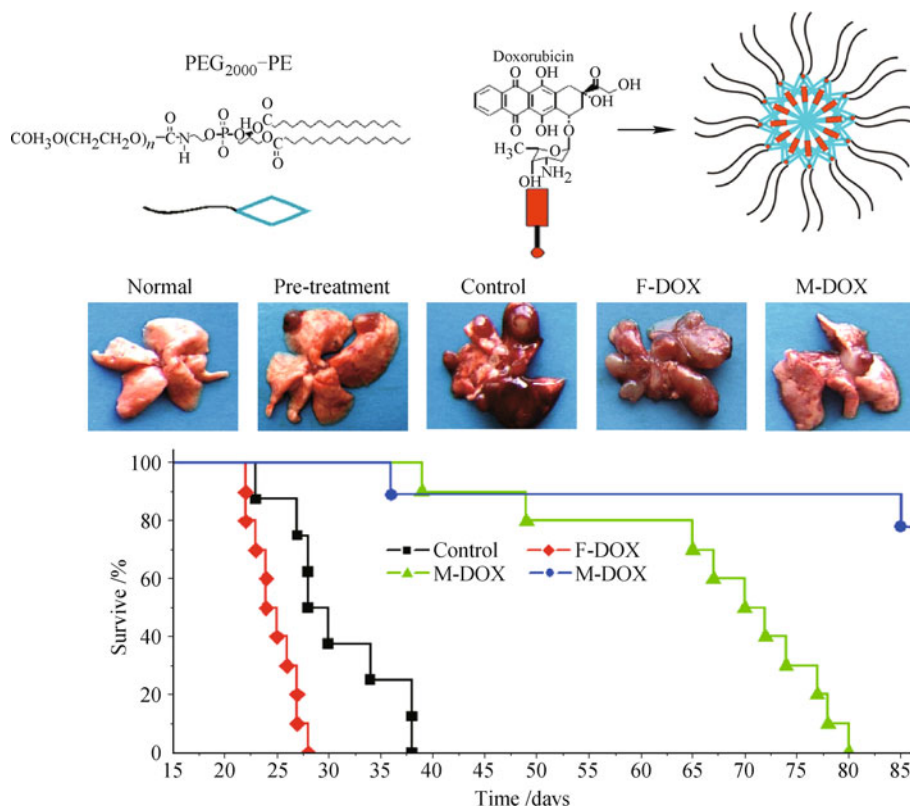


Fig. 10 Schematic illustration of self-assembly of doxorubicin and PEG-PE. Both PEG-PE and doxorubicin are amphiphilic. Upon encapsulation in micelles, the hydrophobic anthracene ring of doxorubicin inserted between the PE phospholipids, with the hydrophilic amino sugar of doxorubicin in the outer shell of the micelle between PEG chains. Antitumor effect of the micelle-encapsulated doxorubicin (M-Dox) in the Lewis lung carcinoma pulmonary model. Mice were injected with free doxorubicin (Free Dox) or M-Dox or empty polyethylene glycol – phosphatidylethanolamine (PEG-PE) micelles as control at day 10 after establishment of tumors. Lungs were harvested at day 24, photograph and survival of mice.

2.7 Nanomaterials and their applications

2.7.1 Molecular nanomagnets

Molecular nanomagnets (MNMs) are the zero or 1D magnetic systems which can exhibit magnet-like behavior originating from individual molecule. MNM provide a wonderful model for understanding the quantum phenomenon in mesoscopic world and has the potential applications in ultra-high density information storage, quantum computing and molecular spintronics. MNMs include cluster-based single-molecule magnets (SMM), single-ion magnets (SIM) and single-chain magnets (SCM). Song Gao *et al.* at Peking University have made important contributions to developing new MNMs. They developed new strategies towards single-chain magnets. For example, they discovered the first homo-spin single-chain magnet in 2003 [89], developed a new route for stringing cluster-based SMMs to SCMs with enhanced uniaxial anisotropy [90], constructed and discovered supramolecular SCMs through spin-canting and non-covalent interactions [91].

Based on his continued work on the external field-dependent magnetic relaxation phenomena in some isolated paramagnetic systems [92, 93], Song Gao *et al.* developed two types of new rare earth single-ion magnets, Dy(acac)₃L and (Cp*)Er(COT), with high anisotropy energy barriers and hysteresis (Fig. 11) [94, 95]. “The discovery of a bona fide organometallic SMM brings the topic of magnetic bistability to a whole new synthetic

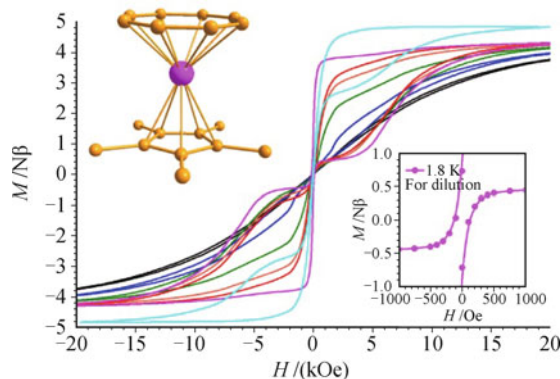


Fig. 11 The Single-Ion Magnet (COT)ErCp*.

audience. The field is now absolutely wide open for new developments.”

In the field of multifunctional molecular magnets, Song Gao *et al.* discovered the coexistence of magnetic and electric orderings in the metal formate frameworks of $[\text{NH}_4][\text{M}(\text{HCOO})_3]$ ($\text{M} = \text{Mn}, \text{Fe}, \text{Co}, \text{Ni}, \text{and Zn}$) [96]. In addition, they developed a facile and effective route to prepare monodisperse magnetic EuS and monodisperse lanthanide oxysulfide nanocrystals by the thermal decomposition of the single molecular precursors under a flow of nitrogen and air, respectively [97, 98].

2.7.2 Carbon based nanomaterials

Carbon based nanomaterial such as carbon nanotubes (CNTs) and graphene are excellent candidates for next generation electronics, arising from their extraordinary performance. Currently, chemical vapor deposition (CVD) is the major stream for the synthesis of these materials. In the last decade, Zhong-Fan Liu *et al.* at Peking University developed a series of CVD growth techniques featured with designing of novel catalysts as well as engineering of growth process. They focused on structure control of CNTs through designing of the CVD process. An important breakthrough is the temperature-mediated growth of single walled carbon nanotubes (SWNTs) [99]. It was once generally believed that the diameter of CNT is solely determined by the size of catalyst. However, this statement is completely refreshed since the modulation of temperature was found to be capable of tuning the diameter of SWNT, resulting in the formation of various nanotube junctions. Another contribution of Zhong-Fan Liu *et al.* toward conductivity control is the direct growth of semiconducting nanotube arrays [100], which is realized through ultraviolet irradiation during the growth process. The as-grown ratio of semiconducting nanotubes could be as high as 95%. Besides, he succeeded in chirality-cloning growth [101] with carbon nanotube segments as seed-like catalyst. They found that the as-grown nanotube strictly followed the chirality of the seed. This achievement paved a novel avenue toward growth of CNTs with identical chirality. Furthermore, diameter-tuned growth was realized with the aid of opened C_{60} caps [102]. When served as catalyst, these narrow distributed carbon shells enabled growth of SWNTs arrays with similar diameter. The designing of carbon catalyst proposed a novel vapor-solid (VS) growth mechanism.

Graphene, a 2D atomic crystal, has attracted worldwide attention since the first sample was exfoliated in 2004 due to its outstanding physical and chemical properties. Challenges to CVD growth of graphene ranged from thickness control to effective doping. In order to

face these challenges, Zhong-Fan Liu *et al.* proposed various means, carried out on both carbon dissolving and non-dissolving substrates. Firstly, he succeeded in segregation growth of graphene by squeezing residual carbon in the carbon dissolving substrate, including Ni, Co and Fe [103]. Uniformity of segregated graphene is greatly improved compared with products from traditional CVD growth. Moreover, nitrogen doped graphene could be produced by incorporation of boron dopants into the nickel substrate [104]. In order to improve the thickness uniformity, binary metal alloy composed was employed as substrate for graphene growth [105]. In addition to traditional catalyst for hydrocarbons (e.g. Ni), another metal with stable carbide (e.g. Mo) was also adopted. During the CVD process, excess carbon was consequently trapped due to carbide formation, leaving only monolayer graphene on the surface. For substrate with negligible carbon solubility (e.g. Cu), growth of graphene occurred solely on the surface, which is terminated once the surface of catalyst is covered. This feature makes it challenging to produce epitaxial structures of graphene, which is essential for potential applications. Van de Waals epitaxy technique was thus introduced to solve this problem. With monolayer graphene as substrate, both topological insulator-graphene heterostructure [106] and bilayer graphene with Bernal stacking [107] were successfully synthesized. Considering the feature of surface growing, a lateral modulation-doping growth technique was later proposed. This allows for the synthesis of mosaic graphene, a patchwork of intrinsic and nitrogen doped graphene connected with single-crystalline junction [108]. It was further proved that as-grown graphene junction is capable of photocurrent generation, facilitated by photothermoelectric effect (Fig. 12). In addition, the surface growth feature was combined with surface steps of substrate during CVD growth, which finally leads to large scale synthesis of graphene nanoribbon arrays [109].

Controllable synthesis of graphene sheets, including layer number, crystallinity, size, edge structure, spatial orientation, etc., is very crucial for further studies and application. Another controllable synthesis of graphene sheets has been reported by Hong-Jun Gao *et al.* at IOPCAS. It is an epitaxially grown method to synthesize a large-scale, highly ordered, continuous, single-crystalline graphene monolayer on Ru(0001) surface [110]. The graphene film shows perfect crystallinity, with good long-range order on the order of millimeters and with no bond breakage, even over the substrate steps. Furthermore, they have developed a method for silicon-layer intercalation between the graphene and Ru(0001) surface. The silicon layers significantly weaken

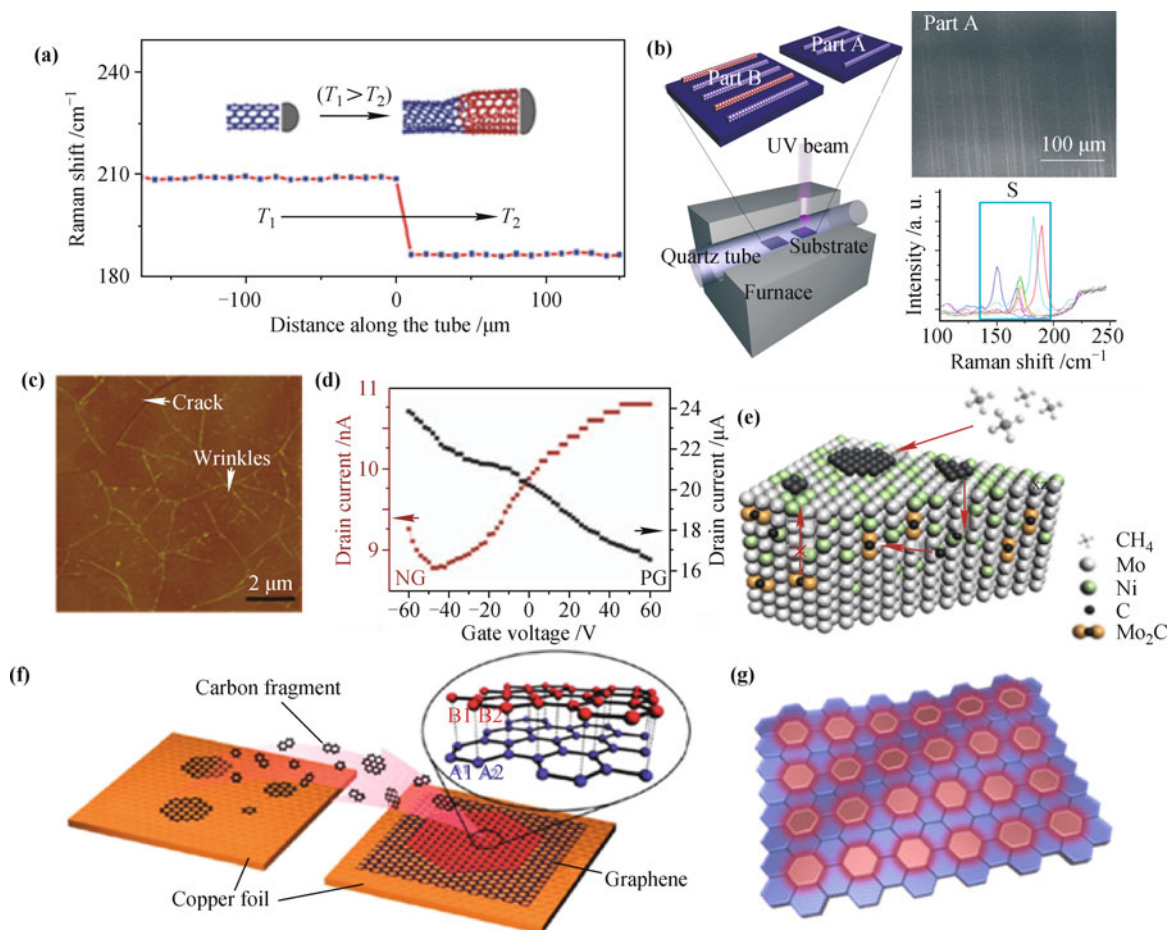


Fig. 12 (a) Temperature-mediated growth of carbon nanotube. The diameter of the tube increased caused by a temperature drop. (b) Direct growth of semiconducting nanotube arrays. Irradiation of ultraviolet light during growth reduced the ratio of metallic tubes. (c) Atomic force microscope image of monolayer graphene by segregation growth. (d) Transport property of segregated nitrogen doped graphene (red), comparing with that of intrinsic graphene (blue). (e) Schematics of growth mechanism involved in binary metal alloy substrate. (f) Schematic drawing of van de Waals epitaxy for bilayer Bernal graphene. (g) Structure of mosaic graphene, with red and blue patches standing for different portions.

the interaction of graphene and the metal substrate but still maintain the graphene's crystallinity, thus achieving electronic decoupling from the metal [111]. The thickness of silicon layer can be atomic controllable for highly doping without the need of chemical doping, which can be used as a top gate [Fig. 13(a)]. The results have shown the potential of incorporating graphene-based structures with Si-based materials and can be very important for future technological progress. Nanolithography technique is a common approach to realize controllable materials synthesis at nano levels. Guang-Yu Zhang *et al.* at IOP-CAS developed a self-aligned anisotropic etching method to fabricate various graphene nanostructures with desired placements, controlled sizes/shapes, such as sub-10 nm wide Z-GNRs, graphene superlattices, triangular graphene islands, etc., and more importantly, with well-defined zigzag edges [Fig. 13(b)] [112]. This approach opens a gateway to experimentally study the rich proper-

ties of zigzag-edged graphene nanostructures, and shows great promise for making future graphene devices or circuits. The metal catalysts in CVD technique play a key role in controllable synthesis of graphene. Yun-Qi Liu *et al.* at ICCAS has introduced a liquid metal catalysts in the CVD process to direct synthesis of uniform single-layered, large-size (up to 10 000 μm^2), spatially self-aligned, and single-crystalline hexagonal graphene flakes (HGFs) and their continuous films [Fig. 13(c)] [113]. These HGFs show an average 2D resistivity of $609 \pm 200 \Omega$ and saturation current density of $0.96 \pm 0.15 \text{ mA}/\mu\text{m}$, demonstrating their good conductivity and capability for carrying high current density. Their results constitute a step forward in the growth and assembly of graphene platelets. Hui-Ming Cheng *et al.* at Institute of Metal Research, Chinese Academy of Sciences (IMRCAS) has used Pt catalysts to grow millimeter-sized hexagonal single-crystal graphene grains and graphene

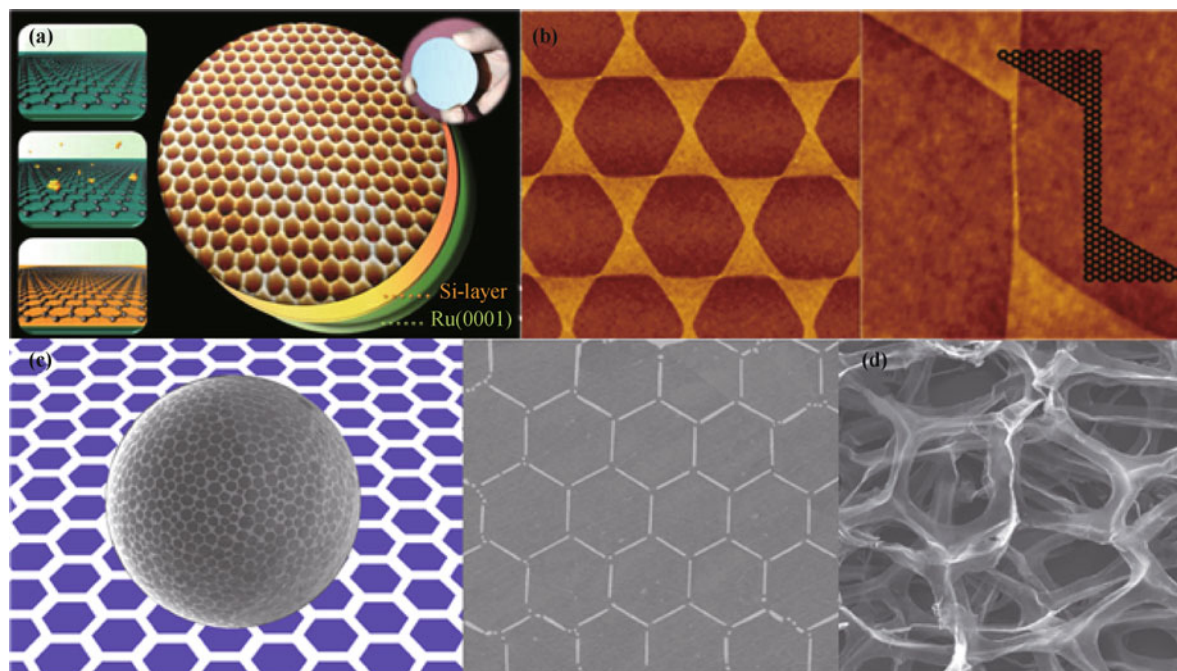


Fig. 13 (a) Silicon layer intercalation of centimeter-scale, epitaxially grown monolayer graphene on Ru(0001); (b) Patterning graphene with zigzag edges by self-aligned anisotropic etching; (c) Uniform hexagonal graphene flakes grown on liquid copper surface; (d) 3D flexible and conductive interconnected graphene networks grown by chemical vapor deposition.

films through ambient-pressure CVD process, and proposed a bubbling method to transfer these single graphene grains and graphene films to arbitrary substrate, which is nondestructive not only to graphene, but also to the Pt substrates [114]. The Pt substrates can be repeatedly used with almost no limit, and the graphene obtained on a repeatedly used Pt substrate has almost the same quality as that obtained originally. The graphene shows high crystalline quality with the reported lowest wrinkle height of 0.8 nm and a carrier mobility of greater than $7100 \text{ cm}^2 \cdot \text{V}^{-1} \cdot \text{s}^{-1}$ under ambient conditions. The repeatable growth of graphene with large single-crystal grains on Pt and its nondestructive transfer may enable various applications. In addition, they have also synthesized graphene foams (GFs) with 3D, conductive all-graphene macrostructures by a template-directed CVD technique using nickel foams as templates [115]. After removing the nickel, they are left with a structure made of a 3D network of interconnected graphene as the fast transport channel of charge carriers for high electrical conductivity [Fig. 13(d)]. Using this unique network structure and the outstanding electrical and mechanical properties of GFs, as an example, they have demonstrated the great potential of GF/poly (dimethyl siloxane) composites for flexible, foldable and stretchable conductors. The unique network structure, high specific surface area and outstanding electrical and mechanical properties of GFs and their composites should enable many applications including high-performance electri-

cally conductive polymer composites, elastic and flexible conductors, electrode materials for lithium ion batteries and supercapacitors, thermal management, catalyst and biomedical supports and so on. They have also demonstrated a thin, lightweight, and flexible lithium ion battery using a 3D flexible and conductive interconnected GF network as both a highly conductive pathway for electrons/lithium ions and light current collector [116]. The battery has shown good flexibility, high capacity, high rate, and long-life cyclic performance even under repeated bending to a small radius of 5 mm.

Special properties and potential applications of graphene-based materials have also attracted extensive attention. Yu-Jie Wei *et al.* at Institute of Mechanics, Chinese Academy of Sciences (IMCAS) has deeply studied how defects affect the mechanic properties of 2D graphene crystal [117]. They found that grain boundary (GB) defects can either strengthen or weaken graphene, which relies on the detailed arrangement of the defects, not just the density of defects. Through both MD simulations and continuum mechanics analysis, the strengths of tilt GBs increase with the square of their tilt angles if pentagon–heptagon defects are evenly spaced. In contrast, the trend breaks down if pentagon–heptagon defects are not evenly distributed. They have also found that mechanical failure always starts from the bond shared by hexagon–heptagon rings in tilted GBs, not the bond that is shared by pentagon–heptagon rings [Fig. 14(a)]. Given that pentagon–heptagon rings are

one of the most common defects in graphene. Raman spectroscopy is a very useful tool to study graphene. Ping-Heng Tan *et al.* at Institute of Semiconductors, Chinese Academy of Sciences (ISCAS) has revealed the interlayer shear mode of few-layer graphene by Raman [118]. They suggest that the corresponding Raman peak measures the interlayer coupling, and the similar shear modes are expected in all 2D layered materials, providing a direct probe of interlayer interactions. Jin Zhang *et al.* at Peking University designed a new kind of surface enhanced Raman spectroscopy (SERS) substrate by introducing plasmonic metal to a graphene layer [119]. Cleaner and more reproducible signals are achieved with a comparable enhancement factor over normal SERS. Thermal conductivity is also a very important property of graphene. Wei-Wei Cai *et al.* at Xiamen University experimentally studied the isotope effects on the thermal properties of graphene [120]. The thermal conductivity, K , of isotopically pure ^{12}C (0.01% ^{13}C) graphene de-

termined by the optothermal Raman technique is higher than $4000 \text{ W}\cdot\text{mK}^{-1}$ at the measured temperature $T_m \sim 320 \text{ K}$, and more than twice higher than that composed of a 50: 50 mixture of ^{12}C and ^{13}C . The experimental results are expected to stimulate further studies aimed at a better understanding of thermal phenomena in 2D crystals. The assembly of graphene is also an attractive issue. Chao Gao *et al.* at Zhejiang University demonstrated that soluble, chemically oxidized graphene or graphene oxide sheets can form chiral liquid crystals in a twist-grain-boundary phase-like model with simultaneous lamellar ordering and long-range helical frustrations [121]. The highly soluble aqueous graphene oxide liquid crystals can be readily spun into meters of continuous and macroscopic fibers [Fig. 14(b)]. After chemical reduction, the integration of high conductivity, excellent mechanical property and unique attributes associated with graphene makes the fibers highly attractive in many applications such as functional textiles and chemical sens-

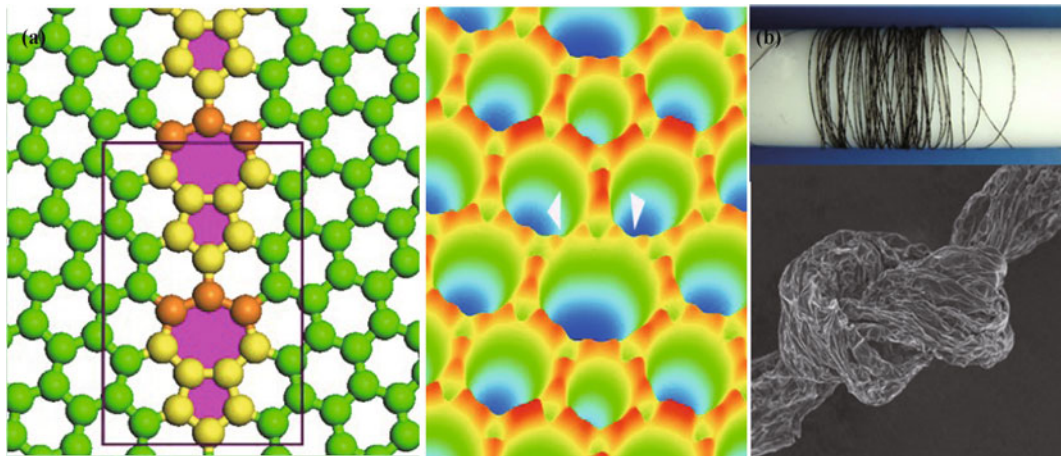


Fig. 14 (a) The nature of strength enhancement and weakening by pentagon-heptagon defects in graphene; (b) Macroscopic assembled graphene fibres.

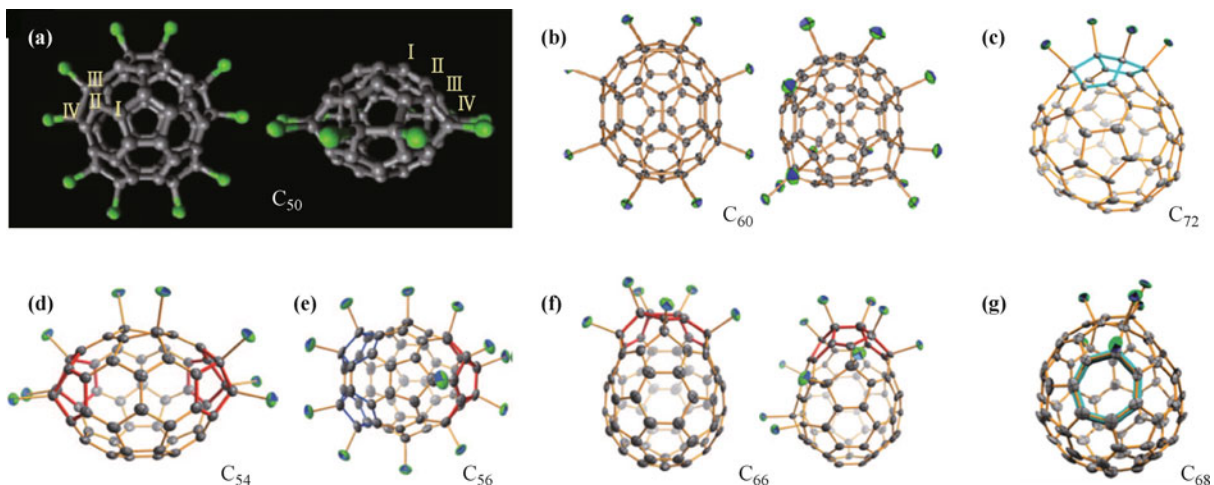


Fig. 15 Different types of non-IPR fullerenes stabilized by exohedral dericatization. (a) C_{50} , (b) C_{60} , (c) C_{72} , (d) C_{54} , (e) C_{56} , (f) C_{66} , (g) C_{68} .

ors. Flexible conducting film is one of the most possible applications for graphene in near future. Gao-Quan Shi *et al.* at Tsinghua University has reported that graphene sheets prepared by the reduction of graphene oxide can be noncovalently functionalized with a water-soluble pyrene derivative, 1-pyrenebutyrate (PB^-), and the resulting PB^- -graphene can be stably dispersed in water [122]. On the basis of this dispersion, large area flexible graphene films have been successfully prepared by filtration. The conductivity of the film is 7 orders of magnitude larger than that of the GO precursor.

Among the carbon-based nanomaterials, fullerenes represent a well-defined type of hollow carbon nanoclusters composed of the strained graphene shells. The isolated pentagon rule (IPR) is widely accepted as a general rule for determining the stability of all-carbon fullerene cages consisting of hexagons and pentagons, in which all the pentagons must be isolated by hexagons. If there is pentagon fusion existing, the local strain inside the fullerenes will be dramatically enhanced, resulting in reduction of their stability. Therefore, fullerenes that violate this rule have been thought of as too reactive to be synthesized because of the presence of the fused pentagons. From 2003 to present, Lan-Sun Zheng *et al.* at Xiamen University have successfully established a novel and general strategy to stabilize the non-IPR fullerenes, namely exohedral derivatization [123]. As shown in Fig. 15, a series of small non-IPR fullerenes including C_{50} [124–126], C_{60} [127], C_{72} [128], C_{54} , C_{56} , C_{66} [129], and C_{68} [130] have been achieved *via* stabilization with different numbers of chlorine atoms. This stabilization of the non-IPR fullerene derivatives is accounted for by the “strain-relief principle” resulting from the rehybridization from sp^2 to sp^3 carbon atoms, as well as the “local aromaticity principle”. The derivatization process with chlorine atoms could give rise to the maintenance of the local aromaticity of the un-derivatized sp^2 carbon skeleton. The experimental availability of these unprecedented non-IPR fullerenes provides many new materials and creative opportunities. Although the chemistry and physics inside the non-IPR fullerenes are still in their infancy, the scientific curiosity of designing and fabricating these nanocluster materials and the realistic requirement of finding unique properties and application potentials promise them a bright future.

2.7.3 Rare earth nanomaterials and fabrication

The rare earth (RE) nanomaterials, which are composed of the lanthanide (Ln) series (from lanthanum to lutetium), yttrium and scandium, can exhibit the sharp fluorescent emission *via* intra- $4f$ or $4f$ – $5d$ transi-

tions with abundant f -orbital configurations. Compared to conventional luminescent materials such as organic fluorescent dyes and inorganic quantum dots (QDs), the RE nanomaterials show unique features including narrow emission band widths (<10 nm), long luminescence lifetime (μs – ms range) and low long-term toxicity.

A variety of chemical techniques, including coprecipitation, thermal decomposition, hydrothermal synthesis, sol-gel processing and combustion synthesis, have been developed to synthesize RE nanocrystals. Some standard methods have been established to obtain RE nanocrystals with tailored crystal sizes, shapes, surface functionalization, chemical composition and optical properties. The excellent work to date for synthesizing RE nanocrystals have been made by many research groups, e.g. Ya-Dong Li, Chun-Hua Yan, Hong-Jie Zhang *et al.* [131–133], as shown in Fig. 16.

Controllable synthesis of nanostructured RE presents the opportunities for fabrication of the catalytic materials with desirable features because these nanomaterials have tunable sizes and specific exposed crystal facets. Ya-Dong Li *et al.* focused in the area of controllable synthesis, assembly, structure, and properties of inorganic nanomaterials over the past decades. They have developed a liquid–solid–solution (LSS) phase transfer and separation strategy for nanocrystal synthesis [134, 135]. In this approach, a water/ethanol mixed solution is used as the main continuous solution phase. Long chain alkyl surfactants like octadecylamine or oleic acid can be used as protecting reagents for the nanocrystals. With this general synthetic procedure, a huge group of monodisperse nanocrystals with sizes in the range of 2–15 nm, which have quite different crystal structures, compositions and properties, have been obtained, including noble metals (Ag, Au, Pd, Pt, Ru, Rh, Ir), magnetic/dielectric (Fe_3O_4 , CoFe_2O_4 , MnFe_2O_4 , ZnFe_2O_4 , BaTiO_3 , SrTiO_3 , etc.), semiconductors (PbS , Ag_2S , CdS , ZnS , ZnSe , CdSe , TiO_2 , ZrO_2 , CuO), rare earth fluorescent (NaYF_4 , YF_3 , LnF_3 , $\text{Ln}(\text{OH})_3$), biomedical ($\text{Ca}_{10}(\text{PO}_4)_6(\text{OH})_2$, CaCO_3), and other monodisperse organic optoelectronic semiconductors (Metal Phthalocyanine), and conducting polymers (PPy and PAN) nanoparticles etc. All these functional nanocrystals obtained through this LSS approach will provide the building blocks for the bottom-up approach to nanoscale fabrication in nanosciences and nanotechnologies.

Besides, they have developed a noble-metal-induced-reduction (NMIR) strategy for bimetallic nanocrystal synthesis [136–139]. In this effective general and convenient synthetic system, octadecylamine (ODA) was selected to serve simultaneously as solvent, surfactant and reducing agent. When noble-metal ions (Au^{3+} , Pd^{2+} ,

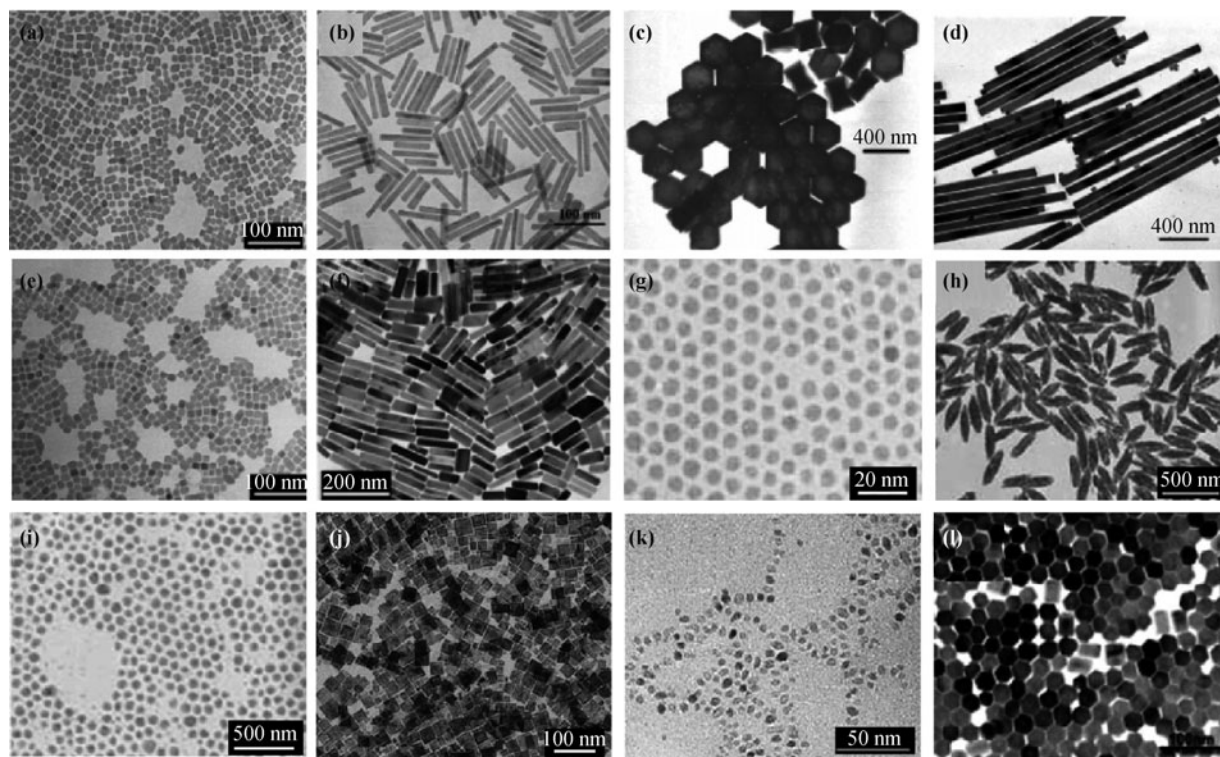


Fig. 16 Typical TEM images of RE nanocrystals (a) NaYF₄:Tb, (b,c) NaYF₄:Eu, (d-f) NaYF₄:Yb-Er, (g) LaF₃, (h) YF₃, (i) YbF₃, (j) LaVO₄:Eu, (k) YBO₃:Eu, and (l) YPO₄·0.8H₂O.

Pt⁴⁺, Ir³⁺, Ru³⁺, Rh³⁺, etc.) and non-noble metal ions (Fe³⁺, Co²⁺, Ni²⁺, Cu²⁺, Zn²⁺, Cd²⁺, In³⁺, Sn²⁺, etc.) coexisted in this system, alloys of noble and non-noble metals could be obtained under controlled conditions. They introduced effective electronegativity ($\chi_{\text{effective}}$) for alloys and regarded them as artificial metal atoms (AMA) which should have the ability to attract electrons to themselves just as single metal atoms do. According to the electronegativity of alloys, a large variety of nanocrystalline intermetallics and alloys with controllable composition, structure, size, and morphology have been successfully synthesized. It is believed that the developed methodology for alloys is of great significance in exploiting low-cost and high-efficiency bimetallic nanocatalysts.

Furthermore, in the field of nanocatalysis, it still remains a great challenge to fully understand the relationship between the catalytic properties (activity, selectivity, and durability) of nanocrystals with their structural characteristics in varied types of reactions. Recognizing the regularity of nanocatalysis and revealing its physical and chemical nature are significant basic issues in catalytic science and technology. According to these basic scientific issues, Ya-Dong Li *et al.* have carried out systematic research work. They proposed the concept of crystal facet-dependent catalytic properties of metal oxide nanocatalysts [140], explained the relationship be-

tween surface defects/oxygen vacancies and the catalytic performance [141], designed supported metal nanocatalysts with novel structures that could relieve the aggregation and detachment of metals [142], comprehended the catalytic mechanism of metal nanoparticles, and investigated the influence of composition, size, morphology, surface atomic arrangement, and surface capping agents of bimetallic nanocatalysts on their catalytic activity, selectivity, and durability (Fig. 17) [143]. In their future work, they will try their best to understand the nature of nanocatalysis in the view of chemical bond and atomic/molecular orbital.

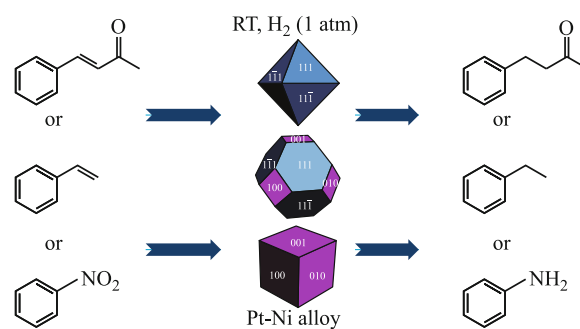


Fig. 17 The structure-property dependence of Pt-Ni nanocrystals in model hydrogenation reactions.

Fabrication of nanomaterial assemblies is an emerging research direction. Currently, the scientists' capability

to assemble nanomaterials is only limited to constructed simple 1D, 2D and 3D structures by taking advantage of different interactions between nanomaterials. Recently, more scientific attentions have been switched from simple to advanced nanomaterial assemblies. For example, Zhi-Yong Tang *et al.* at NCNST found that different types of polydisperse nanoparticles of the size distribution in the range of 20%–30% could self-assemble into monodispersed supraparticles (size distribution is less than 10%) with well-defined core/shell structures (Fig. 18) [144]. This self-limiting growth process is governed by a balance between electrostatic repulsion and van der Waals attraction. The generic nature of the interactions creates flexibility in the composition, size and shape of the constituent nanoparticles, and leads to a large family of self-assembled structures, including hierarchically organized colloidal crystals. In addition to opening the door for fabrication of functional complex nanomaterials, this study can help us to deep understand the formation mechanisms of many organic superstructures, including monodisperse virus particles and polymers.

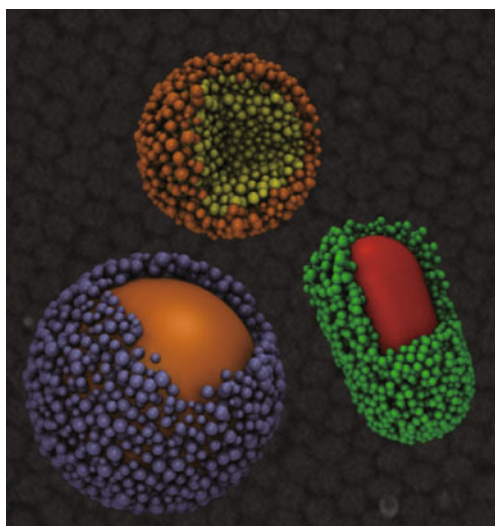


Fig. 18 Scheme of monodisperse supraparticles of different geometries and structures.

2.7.4 Energy nanomaterials

The development of affordable, inexhaustible and clean energy technologies will have huge longer-term benefits. Solar energy, as an alternative to fossil fuels, given its abundance, safety, renewability, and cleanliness, is a promising answer to the global energy crisis. The CAS has launched an initiative to boost the development of solar energy technology since 2008. The initiative motivates the experts to make an action plan and to set up a platform to support the research in solar energy utilization.

As a low-cost photovoltaic technology, organic photovoltaics (OPVs) have been produced by spin-coating or printing techniques [145–147]. By synthesizing new molecules and controlling nanostructures of the active layers, the power conversion efficiency of OPVs can now exceed 9% [148, 149]. During past five years, domestic scientists have made substantial progress in this area. The research is mainly focused on synthesis of new narrow bandgap donor material, including small molecular and polymer donors, and fullerene or non-fullerene acceptors, modification of interface, and control of film morphology. For instance, Yong-Fang Li and Jian-Hui Hou *et al.* reported a series of donor-acceptor type polymers with efficiencies greater than 7% by using two dimensional derivatives as building blocks [150]. They also reported a new fullerene derivative, indene- C_{60} bisadduct (ICBA) with a high efficiency of 7.40% [151, 152]. Yong Cao and Hong-Bin Wu *et al.* successfully demonstrated that simultaneous enhancement in the open circuit voltage, short circuit current density, and fill factor could be achieved in OPVs by simply incorporating a thin layer of alcohol/water-soluble polymer as the cathode interlayer, resulting in an efficiency up to 9.2% [149, 153]. On the other hand, dye sensitized solar cell (DSSC) is a photoelectrochemical system based on a porous layer of semiconductor nanoparticles covered with organic dyes. In the past years, domestic researchers have made great contribution to the fast development of this field. Peng Wang *et al.* produced an iodine-free dye-sensitized solar cell exhibiting an unprecedented power conversion efficiency of 9.4% [154]. Dan Wang *et al.* synthesized multi-shelled ZnO hollow microspheres as photo anode for DSSCs to improve the efficiency of DSSC [155].

As an alternative process of photovoltaic, artificial photosynthesis that splits to generate H_2 and O_2 has also attracted enormous attention as a potential means for the large scale production of H_2 from water using abundant solar light. Jian-Ru Gong *et al.* reported that a high efficiency of the photocatalytic H_2 production was achieved using graphene nanosheets decorated with semiconductor nanoparticles as visible-light-driven photocatalysts [156, 157]. The high photocatalytic H_2 -production activity is attributed predominantly to the presence of graphene, which serves as an electron collector and transporter to efficiently lengthen the lifetime of the photo generated charge carriers from semiconductor nanoparticles.

Among the clean energy technologies, energy storage is a key part for the efficient usage of the harvested energy. Lithium-ion batteries (LIBs) are the most widely used energy storage technology with the advantage of high voltage, high specific energy and long cycle life.

China began the study of LIB at 1980s and much outstanding work has been made. For instance, cathode is one of the key materials and restricts the specific energy of LIB among the component of LIBs. To improve the performance of electrode materials, Yu-Guo Guo *et al.* proposed to incorporate hierarchical carbon network to improve the performance of electrode materials. Because nanocarbon network can afford efficient electron pathway and alleviate stress and volume changes, therefore both kinetic performance and structural stability can be improved [158]. Yong Yang *et al.* synthesized nanostructured $\text{Li}_2\text{FeSiO}_4$ through a hydrothermal-assisted sol-gel process [159]. The $\text{Li}_2\text{FeSiO}_4$ electrode shows a discharge capacity of $160 \text{ mAh}\cdot\text{g}^{-1}$ at C/16 rate, which is of the top international level. On the other hand, some new kinds of anode materials are studied and new strategies are proposed. A series of anode materials with enhanced rate capability and cycling stability were produced by a compositing strategy, including CNT@ TiO_2 coaxial nanocables [160], SnO_2 nanocrystals graphene (SnO_2 -G) composite [161] and Ge@C core-shell nanostructures and reduced graphene oxide nanocomposite (Ge@C/RGO) [162]. Zhao-Wu Tian *et al.* proposed a new carbon-coating technique for electrode materials using nitrogen-containing ionic liquids as precursor [163]. The porous $\text{Li}_4\text{Ti}_5\text{O}_{12}$ uniformly coated with N-doped carbon showed high rate capability and excellent cycling stability. Moreover, the study of mechanism of lithium ions storage in materials is essential to deeply understanding the principle and researching on new materials. Hong Li and coworkers have used an annular-bright-field scanning transmission electron microscopy to image lithium atoms directly in cathode materials LiFePO_4 [164]. It was found that in partially delithiated LiFePO_4 the remaining lithium ions preferably occupy every second layer. This result challenges previously proposed $\text{LiFePO}_4/\text{FePO}_4$ two-phase separation mechanisms.

As an energy storage device with high power density, long cycling life and high reliability, supercapacitor has received growing interest. Carbon material is one kind of supercapacitor materials that is studied most widely. As described previously, Hui-Ming Cheng *et al.* designed a 3D periodic hierarchical porous graphitic carbon (HPGC) that combines macropores, mesoporous walls, and micropores [165]. Macropores act as ion-buffering reservoirs; mesoporous walls provide low-resistant pathways for ions; and micropores strengthen the electric-double-layer capacitance. This new material exhibits high energy and power density. Some transition metal oxides exhibit excellent properties as pseudocapacitive electrode material. Lian Gao *et al.* prepared a manganese dioxide/multi-walled carbon nanotube composite by an

in-situ coating technique. It exhibited a specific capacitance of $250 \text{ F}\cdot\text{g}^{-1}$ [166]. Conducting polymers is another importance candidate for electrode materials with a very high theoretical capacitance. Conducting polymers have been used to prepare composite materials with excellent performance by combining their high capacitance and high cycling stability of carbon materials [167].

2.7.5 Environmental nanomaterials

Environmental pollutions have been increasing threats for China's sustainable growth. Perpetual organic pollutants (POPs), heavy metal species in industrial waste and heavy metal ions in drinking water are three of the most serious issues, causing discomfort, sickness, and even mutations. Nanomaterial based techniques are considered the best solutions to abate the threat from these pollutants.

Jin-Cai Zhao *et al.* at ICCAS developed a TiO_2 based technique, by which many organic dye pollutants could be directly degraded under visible light irradiation, while other more stable organic pollutants could be degraded by co-feeding dye pollutants, which acted as visible light carriers [168]. They developed band gap modification technique as well as facet control technique to modify the TiO_2 catalyst. Modifying the TiO_2 surface further enhanced the separation of photo generated charges for higher efficiency on degradation of organic pollutants. Efficient use of sunlight is the bright spot of this technique [169]. A trial unit has been built by ICCAS researchers for sunlight based degrading of organic pollutants, as shown in Fig. 19(a).

In addition to practical sunlight based devices, Jin-Cai Zhao *et al.* also elucidated the mechanism of photo degradation. With the help of isotopic labeling using ^{18}O -labeled oxygen and water, they were able to pinpoint how oxygen atoms from the green oxidant were inserted into the hydroxyl group in the intermediate species and in the final product [169].

Toxic heavy metal ions such as arsenate, mercury and lead ions have been a health threat to millions of residents in China, whose drinking water sources are contaminated by these ions through either industrial emissions or natural causes. Among several practical techniques, adsorption technique is a convenient method to provide safe drinking water. Wei-Guo Song *et al.* at ICCAS developed a series of nano structured adsorbents, including iron oxide, basic aluminum carbonate, magnesium oxide, etc., which exhibited outstanding adsorption capacities against heavy metal ions in water. The mechanism behind the selective adsorption was also elucidated by synchrotron beam line based spectroscopic technique.



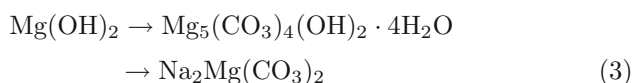
Fig. 19 (a) A trial unit for degrading organic pollutant by sun light; (b) A trial unit to remove arsenate in drink water using combined flocculation and adsorption technique; and (c) A trial unit to remove Cr (VI) from industrial waste by phase transformation.

es, by which the ion exchange between arsenate ions and surface hydroxyl groups on iron oxide [170] or carbonate groups on basic aluminum carbonate [171], and ion exchange between lead ion with surface magnesium cation [172] were confirmed.

Nanomaterial based adsorption technique can be coupled with flocculation technique to achieve best results. Flocculation technique, especially that using nanosized flocculation agent such as Al_{13} , can readily remove most of the heavy metal ions while nanostructured adsorbents can further reduce the heavy metal ion concentration below safe limit. In a recent trial, Chinese researchers from ICCAS and Research Center for Eco-Environmental Sciences, CAS built a combined trial unit [Fig. 19(b)], by which the arsenate concentration was reduced from 110 ppb to 2 ppb.

Solving heavy metal species problems arising from the industrial waste is, however, another technical challenge. For example, the chlorinate industry in China is producing thousands tons of Cr (VI) containing wastes, which is a nasty viscous solid with high Cr (VI) concentration. The difficulty to remove the Cr (VI) is due to the presence of nanoscale $Mg(OH)_2$, which is the main component of the waste. The nano size effect of nano sized $Mg(OH)_2$ lead to strong binding of CrO_4^{2-} to the $Mg(OH)_2$ surface. This is indeed an undesirable effect of nanomaterials. Thus a rational approach is to reverse the nano size effect by increasing the size of $Mg(OH)_2$ to promote the desorption of CrO_4^{2-} .

Zhang Lin *et al.* at Fuzhou Institute of Material Structure, CAS, followed the above approach. They developed an interfacial maneuvering technique to promote fast growth of nano sized $Mg(OH)_2$ particles. With CO_2 as modifier, the nano size $Mg(OH)_2$ particles suspended in water were first induced to aggregate and then grow into large micron sized particles, as the following:



The above phase transformation was fast and reversible. More importantly, with the formation of micron sized $MgCO_3 \cdot 3H_2O$ particles, CrO_4^{2-} anions were released from the original solid $Mg(OH)_2$ nanoparticles, allowing them to be separated from the solid waste [173, 174]. Newly formed $Na_2Mg(CO_3)_2$ particles were free of CrO_4^{2-} contaminate and could be transformed to nano sized $Mg(OH)_2$ as a valuable chemical product [174, 175]. Such technique was successfully applied in a plant in Fujian province of China [Fig. 19(c)] for CrO_4^{2-} waste treatment.

2.8 Nanotechnology for analytical sciences

Electrochemical analysis: Nanomaterials are widely applied in electroanalytical investigations and have good potentials for constructing electrochemical sensing platforms with high sensitivity and selectivity based on different analytical strategies. Electroanalytical analysis based on nanoscience combines characteristics of electrochemistry (e.g., simplicity, speed, high selectivity and high sensitivity) with unique properties of nanomaterials (e.g., electronic, optical, magnetic and catalytic) to become one of the most exciting areas. In order to improve the sensitivity of electrochemical analysis, our scientists reported a series of metal-based hybrid functional nanomaterials for constructing enhanced electrochemical sensing platforms for detecting different molecules [176, 177]. These typical hybrid nanomaterials include CNT/silica coaxial nanocable supported Au/Pt hybrid nanoparticles, polyaniline nanofiber/high-density Pt hybrid nanoparticles, graphene/Pt or Au hybrid nanoparticles and high-density Au/Pt hybrid nanoparticles supported on TiO_2 nanospheres [178].

Graphene nanosheet shows unique electronic, optical, magnetic, thermal and mechanical properties arising from its 2D structure and has many important technical applications. Our electrochemical scientists have taken advantage of the advanced electronic property of this material in electrochemical analysis [179]. The direct elec-

tron transfer (DET) from redox protein to the electrode surface is an important subject in bioelectrochemistry, so graphene nanosheet and its hybrids have been useful in constructing biosensors with proteins. Due to its excellent electrochemical characteristics, graphene nanosheet can be used to carry out immunoassays, small molecule detection, and ions analysis [180, 181]. Thus, the detection system based on graphene nanosheet will be a promising candidate for the sensing device field in the future.

Chromatography and mass spectroscopy with nanomaterials: Proteomic analysis is challenging because of its relatively large population, wide dynamic range, varieties of complexes, and continuous change with time and space. Nanomaterials can enhance the efficient proteolysis of low-level proteins and enable more proteins to be analyzed in a complex biological sample [182]. In proteome research, rapid and effective separation strategies are essential for successful protein identification due to the broad dynamic range of proteins in biological samples. New methods have been developed to carry out proteomic analysis with mass spectrometric analysis. As a novel chromatographic carrier for proteins, nanozeolite has attracted considerable attention due to its large external surface area, high dispersibility in both aqueous and organic solutions, and tunable surface properties. These properties make them promising candidates for the enrichment of trace peptides/proteins [183]. For different peptides, nanozeolites appear not to have apparent discrimination. Meanwhile, all kinds of nanomaterials have been applied in mass spectrometry for enrichment of low-abundance peptides/proteins, such as gold nanoparticles, carbon-derivative nanoparticles, polymers mixed with nanoparticles, and mesoporous materials [184, 185].

Spectrum analysis with nanomaterials: Spectrum analysis is one of the most popular methods to do assays based on its wonderful sensitivity, convenient signal output, low signal-to-noise ratio, easy operation and so on. UV-vis spectra, fluorescence, SERS (Surface-Enhanced Raman Scattering), and SPR (Surface Plasmon Resonance) have been widely applied in chemical and biological analytic areas.

Fluorescent spectrum detection methods are still the predominantly employed detection technologies because of the commercial availability of a wide spectrum of fluorophores, the ease of fluorescent labeling, and the inherent capability for real-time detection. Fluorescent nanoparticles, typical CdSe, CdTe, ZnS etc., exhibit composition- and size-tunable fluorescence throughout the visible to near-infrared range and also provide a relatively high quantum yield and robust stability against

photobleaching. Other fluorescent nanomaterials are also developed vigorously, such as silicon nanoparticles, carbon nanodots, and gold nanoclusters, which have recently been emphasized in analytical areas because of the tunable fluorescence emission, excellent photostability, biocompatibility and low cytotoxicity [186, 187].

Gold nanoparticles (AuNPs) used as a colorimetric reporter rely on their unique SPR property, which causes color changes that result from both scattering and electronic dipole-dipole coupling between neighboring particles. So many kinds of colorimetric detection systems based on AuNPs have been developed and applied in real sample analysis. Significant progresses in the application of AuNPs have been made in chemical and biological analysis [188, 189].

2.9 Nano EHS

With a growing number of innovations in the fields of nanotechnology, engineered nanomaterials with novel physicochemical properties are posing novel challenges in understanding the full spectrum of interactions at the nano-bio interface, including their toxicological aspects. Researchers in Chinese Academy of Sciences proposed and initiated toxicological research of engineered nanomaterials in 2001. Since then, Yu-Liang Zhao and Chun-Ying Chen *et al.* have systematically investigated toxicity properties and their health effects of twelve kinds of engineered nanomaterials including carbon-based nanomaterials, metals and metal oxide nanomaterials, semiconductivity nanomaterials and so on, at different biological levels from cells, tissue, organs to the whole body animals [190–193]. The results disclosed the ability of nanoparticles to cross the biological barriers [194] and enter into the cells and the body. For traditional matter or molecules, nanosize, nanosurface or shape are not the main factors that dominate the important biological processes of cellular uptake. Yu-Liang Zhao *et al.* studied the fate, absorption, distribution, metabolism, excretion and toxicity (ADME/Tox) of metallic (Au, Ag, Fe, Zn, CdSe QDs etc.), metal oxides (TiO₂, SiO₂, ZnO, Fe₂O₃, Fe₃O₄ NPs) based on animal models [190–196]. They found that the size and shape of these nanoparticles always influences the abilities of the NPs on penetrating the biological barriers such as cellular membrane, blood-brain barrier, alveolar-capillary barrier, etc. For example, nanosized copper particles induced gravely toxicological effects and heavy injuries on kidney, liver and spleen of experimental mice, but on a mass basis micro-copper particles did not. Nanosurface is another important factor dominating the toxicity of nanomaterials. For example, protein adsorption of nanoparticles in vivo or in

vitro is an important factor that could change their cellular uptake processes. Because of their huge specific surface area, nanomaterials easily adsorb proteins and small molecules onto their surface, which not only changes the surface features but also affects their toxicity. Protein adsorption induces dynamic changes at the surface during the interaction process. Recently, Yu-Liang Zhao *et al.* revealed the interaction processes between SWCNTs and human blood proteins, fibrinogen, immunoglobulin, albumin, transferrin, and ferritin, using both experimental and theoretical approaches [195, 196]. They found proteins bound to the SWCNT surface with different adsorption capacities and packing modes. More importantly, the competitive binding of blood proteins on the SWCNT surface could greatly alter their cellular interaction pathways and result in much reduced cytotoxicity (Fig. 20). Rapid adsorption of serum protein to the surface of gold nanostructure can also facilitate their cellular uptake and to reduce their cytotoxicity [197, 198].

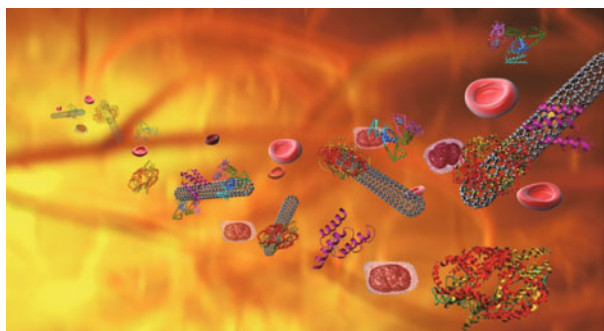


Fig. 20 The competitive binding of blood proteins on the SWCNT surface could greatly alter their cellular interaction pathways and reduce the cytotoxicity of SWCNT.

The origin of toxicity of carbon nanotubes (CNTs) was an open question for a decade and caused worldwide debates on the toxicity and safety issue of CNTs due to the presence of metallic impurities. In addition, the actual desired performance of CNT-based electronics devices can be also largely interfered by these impurities. All these require a reliably advanced quantification method to determine the content of metals in CNTs materials. To this end, Yu-Liang Zhao and Chun-Ying Chen *et al.* successfully established an absolute quantification methodology which can quantify the contribution of metal residues and fiber structure to the toxicity of CNTs [195]. Significant quantities of metal particles could be mobilized from CNTs into surrounding fluids, depending on the properties and constituent of biological microenvironment, as well as the properties of metal particles. Cell viability is highly dependent on the amount of metal residues and iron in particular but not tube structure. The quantitative analytical method they developed

for catalytic metal residues in CNTs has been authorized as the international standard by ISO and IEC, and adopted by their member countries. Moreover, the quantitative nanotoxicity in vivo is another significant contribution Yu-Liang Zhao's group has made for the field, for example, quantitative detection and non-invasive analyses of nanomaterials in vitro and in vivo [199–201]. These findings are crucial for the design of safe nanomaterials, allowing comprehensive reconsideration of nanomaterial impacts on human health during the development of applications of nanotechnologies.

3 Perspectives

In the past decade, we have witnessed the fast development of nanosciences worldwide. We highlighted some progresses of recently fast evolving nanotechnologies in China, most of which we selected in this article showed great potentials in applications. For example, green printing nanotechnology has shown promising prospects in print industry. This new generation printing technique greatly simplifies complicated preparation processes of traditional photolithography method, and significantly prevents discharge of chemical pollutant. It is considered to lead the print industry into a new age of greenization and digitalization. Further application of the green printing technology in other industrial sectors such as building and construction materials, green textiles and printed circuit board (PCB) are developed. All these fields will substantially reduce the pollution problems or energy consumption. To accomplish these, different functional inks and corresponding surfaces have to be developed, which require in-depth knowledge on the surface science, specifically surface wetting and stability of colloidal nanoparticles. For nanophotonic devices based on surface plasmons, the device functions need to be further optimized by employing materials with specific properties and by developing new device fabrication schemes. For plasmonic sensing relying on the electromagnetic field enhancement, the development of substrates with pronounced performances and low cost will be essential for promoting its commercial applications. The development of plasmonics has also attracted the attention of scientists outside of the field, who realized the outstanding properties of surface plasmons being valuable for enhancing the efficiency of optical signal generation and detection, for example, SP-enhanced nonlinear optical processes and SP-enhanced photodetection in graphene devices. Nanomedicine is another fast evolving area which has potentials to address very complicated problems in therapeutics of human diseases like

cancer and infection. However, great challenges for clinical nanomedicine development remain, such as discovery of novel nanomedicine by designs, controllable delivery of drugs to the right place without causing side-effects or inducing drug-resistance, large scale production of manufactured nanoparticles (carriers) with an adequate quality control, translational researches, understanding of the fates of nano carriers in vivo, etc.

More and more inspiring progresses in graphene have been reported since its discovery, in which Chinese researchers have made huge contributions. However, there is still a very long way to realize industrial applications of graphene due to its high cost and structural defects. On nanomaterials, the next research focus should be how to use these nanomaterials in different fields including energy, environment and medicines. Challenges needing to be overcome include decreasing the production cost of nanomaterials and maintaining the unique properties of nanomaterials during industrial applications. Nanotechnologies for energy conversion and storage will keep as one of the hottest topics in China.

Energy-related nanotechnologies play key roles in clean energy area from basic research to application research, aiming to solve the problems for the large-scale applications of clean energy, such as increasing the capacitance of lithium ion batteries and the efficiency of solar cells. In the long term, nanotechnologies will put to full use the next generation energy conversion and storage techniques with high efficiency, low cost and even flexible characteristics. Environmental nanotechnologies are newly emerging area in China. For organic pollutants, catalytic degrading is the ideal route, while for inorganic pollutants, removing them from the environment is perhaps the most practical route. Nanomaterials will be ideal answers for abating both kinds of environmental pollutions. To fully exploit the advantages of nanomaterials in environmental issues, we need to work on the following three fronts: deep understanding of the mechanism of degrading or adsorption; precise and large quantity production of desired nanomaterials at low cost; devices designed for nanomaterials for specific purpose, i.e., reactor for catalytic degrading, vessels for adsorption and desorption.

Analytical science plays an important role in all above areas such as clinical diagnostics, environmental analysis, biochemistry and materials analysis. Modern analytical science aims to pursue the properties of simplicity, speed, selectivity, sensitivity, accuracy, and low costs. Nanomaterials and technologies bring new functions into analytical sensing systems and have made many progresses, such as electrochemical analysis, chromatographic analysis, mass spectrometric analysis, spectrum analysis, and

biochemical sensing and analysis. The development of analytical science should keep close pace and be integrated with the progress of nanotechnologies with the aid of chemists, physicists, biologists and materials scientists.

In China, we will continue our efforts on important research directions of nanotechnology, such as, the controllable fabrication, nano catalysis for chemical industries, bio-inspired nanotechnology in applications, green printing nanotechnology, nano plasmonics, novel nanomedicine, drug delivery system, nanomaterials and their applications, molecular nanomagnets, carbon-based nanomaterials, rare earth nanomaterials, energy nanomaterials, environmental nanomaterials, nanotechnology for analytical sciences, and nano EHS. As we know, nano-standardization is crucial for quality control and to alleviating safety concerns about nanomaterials and nanotechnologies, thus nano-standardization development will have a high priority.

References

1. C. L. Bai, Global voices of science: Ascent of nanoscience in China, *Science*, 2005, 309(5731): 61
2. T. Chen, Q. Chen, X. Zhang, D. Wang, and L. J. Wan, Chiral Kagome network from thiocalix[4]arene tetrasulfonate at the interface of aqueous solution/Au(111) surface: An in situ electrochemical scanning tunneling microscopy study, *J. Am. Chem. Soc.*, 2010, 132(16): 5598
3. S. S. Li, B. H. Northrop, Q. H. Yuan, L. J. Wan, and P. J. Stang, Surface confined metallosupramolecular architectures: Formation and scanning tunneling microscopy characterization, *Acc. Chem. Res.*, 2009, 42(2): 249
4. Q. Chen, T. Chen, G. B. Pan, H. J. Yan, W. G. Song, L. J. Wan, Z. T. Li, Z. H. Wang, B. Shang, L. F. Yuan, and J. L. Yang, Structural selection of graphene supramolecular assembly oriented by molecular conformation and alkyl chain, *Proc. Natl. Acad. Sci. USA*, 2008, 105(44): 16849
5. J. Liu, T. Chen, X. Deng, D. Wang, J. Pei, and L. J. Wan, Chiral hierarchical molecular nanostructures on two-dimensional surface by controllable trinary self-assembly, *J. Am. Chem. Soc.*, 2011, 133(51): 21010
6. L. J. Wan, Fabricating and controlling molecular self-organization at solid surfaces: Studies by scanning tunneling microscopy, *Acc. Chem. Res.*, 2006, 39(5): 334
7. J. S. Hu, Y. G. Guo, H. P. Liang, L. J. Wan, and L. Jiang, Three-dimensional self-organization of supramolecular self-assembled porphyrin hollow hexagonal nanoprisms, *J. Am. Chem. Soc.*, 2005, 127(48): 17090
8. J. S. Hu, L. S. Zhong, W. G. Song, and L. J. Wan, Synthesis of hierarchically structured metal oxides and their application in heavy metal ion removal, *Adv. Mater.*, 2008, 20(15): 2977

9. H. P. Liang, H. M. Zhang, J. S. Hu, Y. G. Guo, L. J. Wan, and C. L. Bai, Pt hollow nanospheres: Facile synthesis and enhanced electrocatalysts, *Angew. Chem. Int. Ed. Engl.*, 2004, 43(12): 1540
10. A. M. Cao, J. S. Hu, H. P. Liang, and L. J. Wan, Self-assembled vanadium pentoxide (V_2O_5) hollow microspheres from nanorods and their application in lithium-ion batteries, *Angew. Chem. Int. Ed. Engl.*, 2005, 44(28): 4391
11. Y. G. Guo, J. S. Hu, and L. J. Wan, Nanostructured materials for electrochemical energy conversion and storage devices, *Adv. Mater.*, 2008, 20(15): 2878
12. X. Sen, Y. G. Guo, and L. J. Wan, Nanocarbon networks for advanced rechargeable lithium batteries, *Acc. Chem. Res.*, 2012, 45(10): 1759
13. S. Xin, L. Gu, N. H. Zhao, Y. X. Yin, L. J. Zhou, Y. G. Guo, and L. J. Wan, Smaller sulfur molecules promise better lithium-sulfur batteries, *J. Am. Chem. Soc.*, 2012, 134(45): 18510
14. Y. Q. Wang, L. Gu, Y. G. Guo, H. Li, X. Q. He, S. Tsukimoto, Y. Ikuhara, and L. J. Wan, Rutile-TiO₂ nanocoating for a high-rate Li₄Ti₅O₁₂ anode of a lithium-ion battery, *J. Am. Chem. Soc.*, 2012, 134(18): 7874
15. D. J. Xue, S. Xin, Y. Yan, K. C. Jiang, Y. X. Yin, Y. G. Guo, and L. J. Wan, Improving the electrode performance of Ge through Ge@C core-shell nanoparticles and graphene networks, *J. Am. Chem. Soc.*, 2012, 134(5): 2512
16. X. L. Pan and X. H. Bao, Reactions over catalysts confined in carbon nanotubes, *Chem. Commun.*, 2008, 47(47): 6271
17. X. L. Pan and X. H. Bao, The effects of confinement inside carbon nanotubes on catalysis, *Acc. Chem. Res.*, 2011, 44(8): 553
18. D. Deng, L. Yu, X. Chen, G. Wang, L. Jin, X. Pan, J. Deng, G. Sun, and X. Bao, Iron encapsulated within pod-like carbon nanotubes for oxygen reduction reaction, *Angew. Chem. Int. Ed.*, 2013, 52(1): 371
19. W. Chen, Z. L. Fan, X. L. Pan, and X. H. Bao, Effect of confinement in carbon nanotubes on the activity of Fischer-Tropsch iron catalyst, *J. Am. Chem. Soc.*, 2008, 130(29): 9414
20. W. Chen, X. L. Pan, and X. H. Bao, Tuning of redox properties of iron and iron oxides via encapsulation within carbon nanotubes, *J. Am. Chem. Soc.*, 2007, 129(23): 7421
21. W. Chen, X. L. Pan, M. G. Willinger, D. S. Su, and X. H. Bao, Facile autoreduction of iron oxide/carbon nanotube encapsulates, *J. Am. Chem. Soc.*, 2006, 128(10): 3136
22. X. L. Pan, Z. L. Fan, W. Chen, Y. J. Ding, H. Y. Luo, and X. H. Bao, Enhanced ethanol production inside carbon-nanotube reactors containing catalytic particles, *Nat. Mater.*, 2007, 6(7): 507
23. Q. Fu, W. X. Li, Yunxi Yao, H. Y. Liu, H. Y. Su, D. Ma, X. K. Gu, L. M. Chen, Z. Wang, H. Zhang, B. Wang, and X. H. Bao, Interface-confined ferrous centers for catalytic oxidation, *Science*, 2010, 328(5982): 1141
24. R. T. Mu, Q. Fu, L. Jin, L. Yu, G. Z. Fang, D. L. Tan, and X. H. Bao, Visualizing chemical reactions confined under graphene, *Angew. Chem. Int. Ed. Engl.*, 2012, 51(20): 4856
25. Q. Fu, F. Yang, and X. H. Bao, Interface-confined oxide nanostructures for catalytic oxidation reactions, *Acc. Chem. Res.*, 2013 (in press)
26. L. Feng, S. Li, Y. Li, H. Li, L. Zhang, J. Zhai, Y. Song, B. Liu, L. Jiang, and D. Zhu, Super-hydrophobic surfaces: from natural to artificial, *Adv. Mater.*, 2002, 14(24): 1857
27. T. Sun, L. Feng, X. F. Gao, and L. Jiang, Bioinspired surfaces with special wettability, *Acc. Chem. Res.*, 2005, 38(8): 644
28. F. Xia and L. Jiang, Bio-inspired, smart, multiscale interfacial materials, *Adv. Mater.*, 2008, 20(15): 2842
29. M. J. Liu, S. T. Wang, Z. X. Wei, Y. L. Song, and L. Jiang, Bioinspired design of a superoleophobic and low adhesive water/solid interface, *Adv. Mater.*, 2009, 21(6): 665
30. Y. M. Zheng, H. Bai, Z. B. Huang, X. L. Tian, F. Q. Nie, Y. Zhao, J. Zhai, and L. Jiang, Directional water collection on wetted spider silk, *Nature*, 2010, 463(7281): 640
31. H. Bai, J. Ju, R. Z. Sun, Y. Chen, Y. M. Zheng, and L. Jiang, Controlled fabrication and water collection ability of bioinspired artificial spider silks, *Adv. Mater.*, 2011, 23(32): 3708
32. X. Hou, W. Guo, and L. Jiang, Biomimetic smart nanopores and nanochannels, *Chem. Soc. Rev.*, 2011, 40(5): 2385
33. W. Guo, L. X. Cao, J. C. Xia, F. Q. Nie, W. Ma, J. M. Xue, Y. L. Song, D. B. Zhu, Y. G. Wang, and L. Jiang, Energy harvesting with single-ion-selective nanopores: A concentration-gradient-driven nanofluidic power source, *Adv. Funct. Mater.*, 2010, 20(8): 1339
34. S. Wang, H. Wang, J. Jiao, K. J. Chen, G. E. Owens, K. I. Kamei, J. Sun, D. J. Sherman, C. P. Behrenbruch, H. Wu, and H. R. Tseng, Three-dimensional nanostructured substrates toward efficient capture of circulating tumor cells, *Angew. Chem. Int. Ed. Engl.*, 2009, 48(47): 8970
35. S. Wang, K. Liu, J. Liu, Z. T. F. Yu, X. Xu, L. Zhao, T. Lee, E. K. Lee, J. Reiss, Y. K. Lee, L. W. K. Chung, J. Huang, M. Rettig, D. Seligson, K. N. Duraiswamy, C. K. F. Shen, and H. R. Tseng, Highly efficient capture of circulating tumor cells by using nanostructured silicon substrates with integrated chaotic micromixers, *Angew. Chem. Int. Ed. Engl.*, 2011, 50(13): 3084
36. L. Chen, X. L. Liu, B. Su, J. Li, L. Jiang, D. Han, and S. T. Wang, Aptamer-mediated efficient capture and release of T lymphocytes on nanostructured surfaces, *Adv. Mater.*, 2011, 23(38): 4376
37. H. B. Yao, Z. H. Tan, H. Y. Fang, and S. H. Yu, Artificial nacre-like bionanocomposite films from the self-assembly of chitosan-montmorillonite hybrid building blocks, *Angew. Chem. Int. Ed. Engl.*, 2010, 49(52): 10127
38. H. B. Yao, H. Y. Fang, Z. H. Tan, L. H. Wu, and S. H. Yu, Biologically inspired, strong, transparent, and functional lay-

- ered organic-inorganic hybrid films, *Angew. Chem. Int. Ed. Engl.*, 2010, 49(12): 2140
39. J. F. Wang, L. Lin, Q. F. Cheng, and L. Jiang, A strong bio-inspired layered PNIPAM-clay nanocomposite hydrogel, *Angew. Chem. Int. Ed. Engl.*, 2012, 51(19): 4676
 40. Y. Demao, Practical Guide of Photosensitive Material and Print Plate, Beijing: Graphic Communications Press, 2007: 53
 41. H. H. Zhou and Y. L. Song, Green plate making technology based on nano-materials, *Adv. Mater. Res.*, 2011, 174: 447
 42. C. Neinhuis and W. Barthlott, Characterization and distribution of water-repellent, self-cleaning plant surfaces, *Ann. Bot.*, 1997, 79(6): 667
 43. X. F. Gao and L. Jiang, Biophysics: Water-repellent legs of water striders, *Nature*, 2004, 432(7013): 36
 44. X. Yao, Y. L. Song, and L. Jiang, Applications of bio-inspired special wettable surfaces, *Adv. Mater.*, 2011, 23(6): 719
 45. R. N. Wenzel, Resistance of solid surfaces to wetting by water, *Ind. Eng. Chem.*, 1936, 28(8): 988
 46. A. B. D. Cassie and S. Baxter, Wettability of porous surfaces, *Trans. Faraday Soc.*, 1944, 40: 546
 47. J. X. Wang, Y. Zhang, S. Wang, Y. L. Song, and L. Jiang, Bioinspired colloidal photonic crystals with controllable wettability, *Acc. Chem. Res.*, 2011, 44(6): 405
 48. Y. Huang, M. Liu, J. X. Wang, J. M. Zhou, L. B. Wang, Y. L. Song, and L. Jiang, Controllable underwater oil-adhesion-interface films assembled from nonspherical particles, *Adv. Funct. Mater.*, 2011, 21(23): 4436
 49. W. L. Barnes, A. Dereux, and T. W. Ebbesen, Surface plasmon subwavelength optics, *Nature*, 2003, 424(6950): 824
 50. Z. Y. Fang, L. R. Fan, C. F. Lin, D. Zhang, A. J. Meixner, and X. Zhu, Plasmonic coupling of bow tie antennas with Ag nanowire, *Nano Lett.*, 2011, 11(4): 1676
 51. X. Guo, M. Qiu, J. M. Bao, B. J. Wiley, Q. Yang, X. N. Zhang, Y. G. Ma, H. K. Yu, and L. M. Tong, Direct coupling of plasmonic and photonic nanowires for hybrid nanophotonic components and circuits, *Nano Lett.*, 2009, 9(12): 4515
 52. Y. R. Fang, Z. P. Li, Y. Z. Huang, S. P. Zhang, P. Nordlander, N. J. Halas, and H. X. Xu, Branched silver nanowires as controllable plasmon routers, *Nano Lett.*, 2010, 10(5): 1950
 53. S. P. Zhang, H. Wei, K. Bao, U. Håkanson, N. J. Halas, P. Nordlander, and H. X. Xu, Chiral surface plasmon polaritons on metallic nanowires, *Phys. Rev. Lett.*, 2011, 107(9): 096801
 54. H. Wei, Z. P. Li, X. R. Tian, Z. X. Wang, F. Z. Cong, N. Liu, S. P. Zhang, P. Nordlander, N. J. Halas, and H. X. Xu, Quantum dot-based local field imaging reveals plasmon-based interferometric logic in silver nanowire networks, *Nano Lett.*, 2011, 11(2): 471
 55. H. Wei, Z. X. Wang, X. R. Tian, M. Käll, and H. X. Xu, Cascaded logic gates in nanophotonic plasmon networks, *Nat. Commun.*, 2011, 2: 387
 56. Y. J. Bao, R. W. Peng, D. J. Shu, M. Wang, X. Lu, J. Shao, W. Lu, and N. B. Ming, Role of interference between localized and propagating surface waves on the extraordinary optical transmission through a subwavelength-aperture array, *Phys. Rev. Lett.*, 2008, 101(8): 087401
 57. X. B. Fan, G. P. Wang, J. C. W. Lee, and C. T. Chan, All-angle broadband negative refraction of metal waveguide arrays in the visible range: Theoretical analysis and numerical demonstration, *Phys. Rev. Lett.*, 2006, 97(7): 073901
 58. H. S. Chen, B. I. Wu, B. Zhang, and J. A. Kong, Electromagnetic wave interactions with a metamaterial cloak, *Phys. Rev. Lett.*, 2007, 99(6): 063903
 59. X. R. Huang, R. W. Peng, and R. H. Fan, Making metals transparent for white light by spoof surface plasmons, *Phys. Rev. Lett.*, 2010, 105(24): 243901
 60. R. H. Fan, R. W. Peng, X. R. Huang, J. Li, Y. Liu, Q. Hu, M. Wang, and X. Zhang, Transparent metals for ultrabroadband electromagnetic waves, *Adv. Mater.*, 2012, 24(15): 1980
 61. S. L. Sun, Q. He, S. Y. Xiao, Q. Xu, X. Li, and L. Zhou, Gradient-index meta-surfaces as a bridge linking propagating waves and surface waves, *Nat. Mater.*, 2012, 11(5): 426
 62. Y. H. Chen, L. Huang, L. Gan, and Z. Y. Li, Wavefront shaping of infrared light through a subwavelength hole, *Light: Science & Applications*, 2012, 1(8): e26
 63. L. Li, T. Li, S. M. Wang, C. Zhang, and S. N. Zhu, Plasmonic Airy beam generated by in-plane diffraction, *Phys. Rev. Lett.*, 2011, 107(12): 126804
 64. H. X. Xu, E. J. Bjerneld, M. Käll, and L. Borjesson, Spectroscopy of single hemoglobin molecules by surface enhanced raman scattering, *Phys. Rev. Lett.*, 1999, 83(21): 4357
 65. Z. Q. Tian, B. Ren, and D. Y. Wu, Surface-enhanced raman scattering: from noble to transition metals and from rough surfaces to ordered nanostructures, *J. Phys. Chem. B*, 2002, 106(37): 9463
 66. J. F. Li, Y. F. Huang, Y. Ding, Z. L. Yang, S. B. Li, X. S. Zhou, F. R. Fan, W. Zhang, Z. Y. Zhou, Y. Wu, B. Ren, Z. L. Wang, and Z. Q. Tian, Shell-isolated nanoparticle-enhanced Raman spectroscopy, *Nature*, 2010, 464(7287): 392
 67. H. Wei, F. Hao, Y. Huang, W. Wang, P. Nordlander, and H. Xu, Polarization dependence of surface-enhanced Raman scattering in gold nanoparticle-nanowire systems, *Nano Lett.*, 2008, 8(8): 2497
 68. H. Wei, U. Håkanson, Z. L. Yang, F. Höök, and H. X. Xu, Individual nanometer hole-particle pairs for surface-enhanced Raman scattering, *Small*, 2008, 4(9): 1296
 69. H. Y. Liang, Z. P. Li, W. Z. Wang, Y. S. Wu, and H. X. Xu, Highly surface-roughened flower-like silver nanoparticles for extremely sensitive substrates of surface-enhanced Raman scattering, *Adv. Mater.*, 2009, 21(45): 4614
 70. Y. R. Fang, H. Wei, F. Hao, P. Nordlander, and H. X. Xu, Remote-excitation surface-enhanced Raman scattering using propagating Ag nanowire plasmons, *Nano Lett.*, 2009, 9(5): 2049

71. M. T. Sun, Z. Zhang, H. Zheng, and H. X. Xu, In-situ plasmon-driven chemical reactions revealed by high vacuum tip-enhanced Raman spectroscopy, *Scientific Reports*, 2012, 2: 647
72. Z. Liu, S. Y. Ding, Z. B. Chen, X. Wang, J. H. Tian, J. R. Anema, X. S. Zhou, D. Y. Wu, B. W. Mao, X. Xu, B. Ren, and Z. Q. Tian, Revealing the molecular structure of single-molecule junctions in different conductance states by fishing-mode tip-enhanced Raman spectroscopy, *Nat. Commun.*, 2011, 2: 305
73. C. Y. Chen, G. M. Xing, J. X. Wang, Y. L. Zhao, B. Li, J. Tang, G. Jia, T. C. Wang, J. Sun, L. Xing, H. Yuan, Y. X. Gao, H. Meng, Z. Chen, F. Zhao, Z. F. Chai, and X. H. Fang, Multihydroxylated $[\text{Gd}@C_{82}(\text{OH})_{22}]_n$ nanoparticles: Antineoplastic activity of high efficiency and low toxicity, *Nano Lett.*, 2005, 5(10): 2050
74. X. J. Liang, H. Meng, Y. Wang, H. Y. He, J. Meng, J. Lu, P. C. Wang, Y. Zhao, X. Gao, B. Sun, C. Y. Chen, G. Xing, D. Shen, M. M. Gottesman, Y. Wu, J. J. Yin, and L. Jia, Metallofullerene nanoparticles circumvent tumor resistance to cisplatin by reactivating endocytosis, *Proc. Natl. Acad. Sci. USA*, 2010, 107(16): 7449
75. S. G. Kang, G. Q. Zhou, P. Yang, Y. Liu, B. Y. Sun, T. Huynh, H. Meng, L. N. Zhao, G. M. Xing, C. Y. Chen, Y. L. Zhao, and R. H. Zhou, Molecular mechanism of pancreatic tumor metastasis inhibition by $\text{Gd}@C_{82}(\text{OH})_{22}$ and its implication for de novo design of nanomedicine, *Proc. Natl. Acad. Sci. USA*, 2012, 109(38): 15431
76. X. W. Ma, Y. L. Zhao, and X. J. Liang, Theranostic nanoparticles engineered for clinic and pharmaceuticals, *Acc. Chem. Res.*, 2011, 44(10): 1114
77. J. Tang, G. M. Xing, Y. L. Zhao, L. Jing, X. F. Gao, Y. Cheng, H. Yuan, F. Zhao, Z. Chen, H. Meng, H. Zhang, H. J. Qian, R. Su, and K. Ibrahim, Periodical variation of electronic properties in polyhydroxylated metallofullerene materials, *Adv. Mater.*, 2006, 18(11): 1458
78. L. Yan, Y. B. Zheng, F. Zhao, S. J. Li, X. F. Gao, B. Q. Xu, P. S. Weiss, and Y. L. Zhao, Chemistry and physics of a single atomic layer: Strategies and challenges for functionalization of graphene and graphene-based materials, *Chem. Soc. Rev.*, 2012, 41(1): 97
79. H. Meng, G. M. Xing, B. Y. Sun, F. Zhao, H. Lei, W. Li, Y. Song, and Z. Chen, H. Yuan, X. X. Wang, J. Long, C. Y. Chen, X. J. Liang, N. Zhang, Z. F. Chai, and Y. L. Zhao, Potent Angiogenesis Inhibition by the Particulate Form of Fullerene Derivatives, *ACS Nano*, 2010, 4(5): 2773
80. D. Yang, Y. L. Zhao, H. Guo, Y. N. Li, P. Tewary, G. M. Xing, W. Hou, J. J. Oppenheim, and N. Zhang, $[\text{Gd}@C_{82}(\text{OH})_{22}]_n$ nanoparticles induce dendritic cell maturation and activate Th1 immune responses, *ACS Nano*, 2010, 4(2): 1178
81. H. Meng, G. M. Xing, E. Blanco, Y. Song, L. Zhao, B. Y. Sun, X. Li, P. C. Wang, A. Korotcov, W. Li, X. J. Liang, and C. Y. Yuan, H. Chen, F. Zhao, Z. Chen, T. Sun, Z. F. Chai, M. Ferrari, and Y. L. Zhao, Gadolinium metallofullerenol nanoparticles inhibit cancer metastasis through matrix metalloproteinase inhibition: imprisoning instead of poisoning cancer cells, *Nanomedicine: Nanotechnology, Biology and Medicine*, 2012, 8(2): 136
82. M. J. Bissell and D. Radisky, Putting tumours in context, *Nat. Rev. Cancer*, 2001, 1(1): 46
83. R. Duncan, Polymer conjugates as anticancer nanomedicines, *Nat. Rev. Cancer*, 2006, 6(9): 688
84. N. Tang, G. Du, N. Wang, C. Liu, H. Hang, and W. Liang, Improving penetration in tumors with nanoassemblies of phospholipids and doxorubicin, *J. Natl. Cancer Inst.*, 2007, 99(13): 1004
85. X. Lu, F. Zhang, L. Qin, F. Xiao, and W. Liang, Polymeric micelles as a drug delivery system enhance cytotoxicity of vinorelbine through more intercellular accumulation, *Drug Deliv.*, 2010, 17(4): 255
86. Y. Wang, R. Wang, X. Lu, W. Lu, C. Zhang, and W. Liang, Pegylated phospholipids-based self-assembly with water-soluble drugs, *Pharm. Res.*, 2010, 27(2): 361
87. J. Wang, Y. Wang, and W. Liang, Delivery of drugs to cell membranes by encapsulation in PEG-PE micelles, *J. Control. Release*, 2012, 160(3): 637
88. J. Wang, H. Qu, L. Jin, W. Zeng, L. Qin, F. Zhang, X. Wei, W. Lu, C. Zhang, and W. Liang, Pegylated phosphotidylethanolamine inhibiting P-glycoprotein expression and enhancing retention of doxorubicin in MCF7/ADR cells, *J. Pharm. Sci.*, 2011, 100(6): 2267
89. T. F. Liu, D. Fu, S. Gao, Y. Z. Zhang, H. L. Sun, G. Su, and Y. J. Liu, An azide-bridged homospin single-chain magnet: $[\text{Co}(2,2'\text{-bithiazoline})(\text{N}_3)_2]_n$, *J. Am. Chem. Soc.*, 2003, 125(46): 13976
90. H. B. Xu, B. W. Wang, F. Pan, Z. M. Wang, and S. Gao, Stringing oxo-centered trinuclear $[\text{MnIII}_3\text{O}]$ units into single-chain magnets with formate or azide linkers, *Angew. Chem. Int. Ed. Engl.*, 2007, 46(39): 7388
91. M. Ding, B. Wang, Z. Wang, J. Zhang, O. Fuhr, D. Fenske, and S. Gao, Constructing single-chain magnets by supramolecular - stacking and spin canting: A case study on manganese (III) corroles, *Chemistry*, 2012, 18(3): 915
92. B. Q. Ma, S. Gao, G. Su, and G. X. Xu, Cyano-bridged 4f-3d coordination polymers with a unique two-dimensional topological architecture and unusual magnetic behavior, *Angew. Chem. Int. Ed. Engl.*, 2001, 40(2): 434
93. S. Gao, G. Su, T. Yi, and B. Q. Ma, Observation of an unusual field-dependent slow magnetic relaxation and two distinct transitions in a family of rare-earth - transition-metal complexes, *Phys. Rev. B*, 2001, 63(5): 054431
94. S. D. Jiang, B. W. Wang, G. Su, Z. M. Wang, and S. Gao, A mononuclear dysprosium complex featuring single-molecule-magnet behavior, *Angew. Chem. Int. Ed. Engl.*, 2010, 49(41): 7448
95. S. D. Jiang, B. W. Wang, H. L. Sun, Z. M. Wang, and S.

- Gao, An organometallic single-ion magnet, *J. Am. Chem. Soc.*, 2011, 133(13): 4730
96. G. C. Xu, W. Zhang, X. M. Ma, Y. H. Chen, L. Zhang, H. L. Cai, Z. M. Wang, R. G. Xiong, and S. Gao, Coexistence of magnetic and electric orderings in the metal-formate frameworks of $[\text{NH}_4][\text{M}(\text{HCOO})_3]$, *J. Am. Chem. Soc.*, 2011, 133(38): 14948
 97. F. Zhao, M. Yuan, W. Zhang, and S. Gao, Monodisperse lanthanide oxysulfide nanocrystals, *J. Am. Chem. Soc.*, 2006, 128(36): 11758
 98. F. Zhao, H. L. Sun, G. Su, and S. Gao, Synthesis and size-dependent magnetic properties of monodisperse EuS nanocrystals, *Small*, 2006, 2(2): 244
 99. Y. G. Yao, Q. W. Li, J. Zhang, R. Liu, L. Y. Jiao, Y. T. Zhu, and Z. F. Liu, Temperature-mediated growth of single-walled carbon-nanotube intramolecular junctions, *Nat. Mater.*, 2007, 6(4): 283
 100. G. Hong, B. Zhang, B. H. Peng, J. Zhang, W. M. Choi, J. Y. Choi, J. M. Kim, and Z. F. Liu, Direct growth of semiconducting single-walled carbon nanotube array, *J. Am. Chem. Soc.*, 2009, 131(41): 14642
 101. Y. G. Yao, C. Q. Feng, J. Zhang, and Z. F. Liu, "Cloning" of single-walled carbon nanotubes via open-end growth mechanism, *Nano Lett.*, 2009, 9(4): 1673
 102. X. Yu, J. Zhang, W. Choi, J. Y. Choi, J. M. Kim, L. Gan, and Z. Liu, Cap formation engineering: from opened C60 to single-walled carbon nanotubes, *Nano Lett.*, 2010, 10(9): 3343
 103. N. Liu, L. Fu, B. Y. Dai, K. Yan, X. Liu, R. Q. Zhao, Y. F. Zhang, and Z. F. Liu, Universal segregation growth approach to wafer-size graphene from non-noble metals, *Nano Lett.*, 2010, 11(1): 297
 104. C. Zhang, L. Fu, N. Liu, M. Liu, Y. Wang, and Z. F. Liu, Synthesis of nitrogen-doped graphene using embedded carbon and nitrogen sources, *Adv. Mater.*, 2011, 23(8): 1020
 105. B. Dai, L. Fu, Z. Zou, M. Wang, H. Xu, S. Wang, and Z. Liu, Rational design of a binary metal alloy for chemical vapour deposition growth of uniform single-layer graphene, *Nat. Commun.*, 2011, 2: 522
 106. W. H. Dang, H. L. Peng, H. Li, P. Wang, and Z. F. Liu, Epitaxial heterostructures of ultrathin topological insulator nanoplate and graphene, *Nano Lett.*, 2010, 10(8): 2870
 107. K. Yan, H. L. Peng, Y. Zhou, H. Li, and Z. F. Liu, Formation of bilayer bernal graphene: layer-by-layer epitaxy via chemical vapor deposition, *Nano Lett.*, 2011, 11(3): 1106
 108. K. Yan, D. Wu, H. Peng, L. Jin, Q. Fu, X. Bao, and Z. Liu, Modulation-doped growth of mosaic graphene with single-crystalline p-n junctions for efficient photocurrent generation, *Nat. Commun.*, 2012, 3: 1280
 109. Z. H. Pan, N. Liu, L. Fu, and Z. F. Liu, Wrinkle engineering: A new approach to massive graphene nanoribbon arrays, *J. Am. Chem. Soc.*, 2011, 133(44): 17578
 110. Y. Pan, H. G. Zhang, D. X. Shi, J. T. Sun, S. X. Du, F. Liu, and H. J. Gao, Highly ordered, millimeter-scale, continuous, single-crystalline graphene monolayer formed on Ru (0001), *Adv. Mater.*, 2009, 21(27): 2777
 111. J. H. Mao, L. Huang, Y. Pan, M. Gao, J. F. He, H. T. Zhou, H. M. Guo, Y. Tian, Q. Zou, L. Z. Zhang, H. G. Zhang, Y. L. Wang, S. X. Du, X. J. Zhou, A. H. C. Neto, and H. J. Gao, Silicon layer intercalation of centimeter-scale, epitaxially grown monolayer graphene on Ru(0001), *Appl. Phys. Lett.*, 2012, 100(9): 093101
 112. Z. W. Shi, R. Yang, L. C. Zhang, Y. Wang, D. H. Liu, D. X. Shi, E. G. Wang, and G. Y. Zhang, Patterning graphene with zigzag edges by self-aligned anisotropic etching, *Adv. Mater.*, 2011, 23(27): 3061
 113. D. C. Geng, B. Wu, Y. L. Guo, L. P. Huang, Y. Z. Xue, J. Y. Chen, G. Yu, L. Jiang, W. P. Hu, and Y. Q. Liu, Uniform hexagonal graphene flakes and films grown on liquid copper surface, *Proc. Natl. Acad. Sci. USA*, 2012, 109(21): 7992
 114. L. B. Gao, W. C. Ren, H. L. Xu, L. Jin, Z. X. Wang, T. Ma, L. P. Ma, Z. Y. Zhang, Q. Fu, L. M. Peng, X. H. Bao, and H. M. Cheng, Repeated growth and bubbling transfer of graphene with millimetre-size single-crystal grains using platinum, *Nat. Commun.*, 2012, 3: 699
 115. Z. P. Chen, W. C. Ren, L. B. Gao, B. L. Liu, S. F. Pei, and H. M. Cheng, Three-dimensional flexible and conductive interconnected graphene networks grown by chemical vapour deposition, *Nat. Mater.*, 2011, 10(6): 424
 116. N. Li, Z. P. Chen, W. C. Ren, F. Li, and H. M. Cheng, Flexible graphene-based lithium ion batteries with ultrafast charge and discharge rates, *Proc. Natl. Acad. Sci. USA*, 2012, 109(43): 17360
 117. Y. J. Wei, J. T. Wu, H. Q. Yin, X. H. Shi, R. G. Yang, and M. Dresselhaus, The nature of strength enhancement and weakening by pentagon-heptagon defects in graphene, *Nat. Mater.*, 2012, 11(9): 759
 118. P. H. Tan, W. P. Han, W. J. Zhao, Z. H. Wu, K. Chang, H. Wang, Y. F. Wang, N. Bonini, N. Marzari, N. Pugno, G. Savini, A. Lombardo, and A. C. Ferrari, The shear mode of multilayer graphene, *Nat. Mater.*, 2012, 11(4): 294
 119. W. G. Xu, X. Ling, J. Q. Xiao, M. S. Dresselhaus, J. Kong, H. X. Xu, Z. F. Liu, and J. Zhang, Surface enhanced Raman spectroscopy on a flat graphene surface, *Proc. Natl. Acad. Sci. USA*, 2012, 109(24): 9281
 120. S. S. Chen, Q. Z. Wu, C. Mishra, J. Y. Kang, H. J. Zhang, K. Cho, W. W. Cai, A. A. Balandin, and R. S. Ruoff, Thermal conductivity of isotopically modified graphene, *Nat. Mater.*, 2012, 11(3): 203
 121. Z. Xu and C. Gao, Graphene chiral liquid crystals and macroscopic assembled fibres, *Nat. Commun.*, 2011, 2: 571
 122. Y. X. Xu, H. Bai, G. W. Lu, C. Li, and G. Q. Shi, Flexible graphene films via the filtration of water-soluble noncovalent functionalized graphene sheets, *J. Am. Chem. Soc.*, 2008, 130(18): 5856
 123. Y. Z. Tan, S. Y. Xie, R. B. Huang, and L. S. Zheng, The stabilization of fused-pentagon fullerene molecules, *Nat. Chem.*, 2009, 1(6): 450

124. S. Y. Xie, F. Gao, X. Lu, R. B. Huang, C. R. Wang, X. Zhang, M. L. Liu, S. L. Deng, and L. S. Zheng, Capturing the labile fullerene[50] as $C_{50}Cl_{10}$, *Science*, 2004, 304(5671): 699
125. X. Lu, Z. Chen, W. Thiel, P. Schleyer, R. B. Huang, and L. S. Zheng, Properties of fullerene[50] and D5h decachlorofullerene[50]: A computational study, *J. Am. Chem. Soc.*, 2004, 126(45): 14871
126. X. Han, S. J. Zhou, Y. Z. Tan, X. Wu, F. Gao, Z. J. Liao, R. B. Huang, Y. Q. Feng, X. Lu, S. Y. Xie, and L. S. Zheng, Crystal structures of saturn-like $C_{50}Cl_{10}$ and pineapple-shaped $C_{64}Cl_4$: geometric implications of double- and triple-pentagon-fused chlorofullerenes, *Angew. Chem. Int. Ed.*, 2008, 47(29): 5340
127. Y. Z. Tan, Z. J. Liao, Z. Z. Qian, R. T. Chen, X. Wu, H. Liang, X. Han, F. Zhu, S. J. Zhou, Z. Zheng, X. Lu, S. Y. Xie, R. B. Huang, and L. S. Zheng, Two I(h)-symmetry-breaking C_{60} isomers stabilized by chlorination, *Nat. Mater.*, 2008, 7(10): 790
128. Y. Z. Tan, T. Zhou, J. Bao, G. J. Shan, S. Y. Xie, R. B. Huang, and L. S. Zheng, $C_{72}Cl_4$: A pristine fullerene with favorable pentagon-adjacent structure, *J. Am. Chem. Soc.*, 2010, 132(48): 17102
129. Y. Z. Tan, J. Li, F. Zhu, X. Han, W. S. Jiang, R. B. Huang, Z. Zheng, Z. Z. Qian, R. T. Chen, Z. J. Liao, S. Y. Xie, X. Lu, and L. S. Zheng, Chlorofullerenes featuring triple sequentially fused pentagons, *Nat. Chem.*, 2010, 2(4): 269
130. Y. Z. Tan, R. T. Chen, Z. J. Liao, J. Li, F. Zhu, X. Lu, S. Y. Xie, J. Li, R. B. Huang, and L. S. Zheng, Carbon arc production of heptagon-containing fullerene[68], *Nat. Commun.*, 2011, 2: 420
131. X. W. Liu, D. S. Wang, and Y. D. Li, Synthesis and catalytic properties of bimetallic nanomaterials with various architectures, *Nano Today*, 2012, 7(5): 448
132. R. Si, Y. W. Zhang, L. P. You, and C. H. Yan, Rare-earth oxide nanopolyhedra, nanoplates, and nanodisks, *Angew. Chem. Int. Ed. Engl.*, 2005, 44(21): 3256
133. W. D. Shi, J. B. Yu, H. S. Wang, and H. J. Zhang, Hydrothermal synthesis of single-crystalline antimony telluride nanobelts, *J. Am. Chem. Soc.*, 2006, 128(51): 16490
134. X. Wang, J. Zhuang, Q. Peng, and Y. D. Li, A general strategy for nanocrystal synthesis, *Nature*, 2005, 437(7055): 121
135. X. Wang, Q. Peng, and Y. D. Li, Interface-mediated growth of monodispersed nanostructures, *Acc. Chem. Res.*, 2007, 40(8): 635
136. D. S. Wang and Y. D. Li, One-pot protocol for Au-based hybrid magnetic nanostructures via a noble-metal-induced reduction process, *J. Am. Chem. Soc.*, 2010, 132(18): 6280
137. D. S. Wang, Q. Peng, and Y. D. Li, Nanocrystalline intermetallics and alloys, *Nano Res.*, 2010, 3(8): 574
138. D. S. Wang and Y. D. Li, Bimetallic nanocrystals: Liquid-phase synthesis and catalytic applications, *Adv. Mater.*, 2011, 23(9): 1044
139. D. S. Wang, P. Zhao, and Y. D. Li, General preparation for Pt-based alloy nanoporous nanoparticles as potential nanocatalysts, *Scientific Reports*, 2011, 1: 37
140. K. B. Zhou, X. Wang, X. M. Sun, Q. Peng, and Y. D. Li, Enhanced catalytic activity of ceria nanorods from well-defined reactive crystal planes, *J. Catal.*, 2005, 229(1): 206
141. X. W. Liu, K. B. Zhou, L. Wang, B. Y. Wang, and Y. D. Li, Oxygen vacancy clusters promoting reducibility and activity of ceria nanorods, *J. Am. Chem. Soc.*, 2009, 131(9): 3140
142. C. Chen, C. Y. Nan, D. S. Wang, Q. Su, H. H. Duan, X. W. Liu, L. S. Zhang, D. R. Chu, W. G. Song, Q. Peng, and Y. D. Li, Mesoporous multicomponent nanocomposite colloidal spheres: ideal high-temperature stable model catalysts, *Angew. Chem. Int. Ed. Engl.*, 2011, 50(16): 3725
143. Y. E. Wu, S. F. Cai, D. S. Wang, W. He, and Y. D. Li, Syntheses of water-soluble octahedral, truncated octahedral, and cubic Pt-Ni nanocrystals and their structure-activity study in model hydrogenation reactions, *J. Am. Chem. Soc.*, 2012, 134(21): 8975
144. Y. Xia, T. D. Nguyen, M. Yang, B. Lee, A. Santos, P. Podsiadlo, Z. Tang, S. C. Glotzer, and N. A. Kotov, Self-assembly of self-limiting monodisperse supraparticles from polydisperse nanoparticles, *Nat. Nanotechnol.*, 2011, 6(9): 580
145. J. W. Chen and Y. Cao, Development of novel conjugated donor polymers for high-efficiency bulk-heterojunction photovoltaic devices, *Acc. Chem. Res.*, 2009, 42 (11): 1709
146. L. J. Huo and J. H. Hou, Benzo[1,2-b:4,5-b']dithiophene-based conjugated polymers: band gap and energy level control and their application in polymer solar cells, *Polym. Chem.*, 2011, 2 (11): 2453
147. Y. F. Li, Molecular design of photovoltaic materials for polymer solar cells: toward suitable electronic energy levels and broad absorption, *Acc. Chem. Res.*, 2012, 45(5): 723
148. H. Y. Chen, J. H. Hou, S. Q. Zhang, Y. Y. Liang, G. W. Yang, Y. Yang, L. P. Yu, Y. Wu, and G. Li, Polymer solar cells with enhanced open-circuit voltage and efficiency, *Nat. Photon.*, 2009, 3 (11): 649
149. Z. C. He, C. M. Zhong, C. M. Su, M. Xu, H. B. Wu, and Y. Cao, Enhanced power-conversion efficiency in polymer solar cells using an inverted device structure, *Nat. Photon.*, 2012, 6(9): 591
150. L. J. Huo, S. Q. Zhang, X. Guo, F. Xu, Y. F. Li, and J. H. Hou, Replacing alkoxy groups with alkylthienyl groups: a feasible approach to improve the properties of photovoltaic polymers, *Angew. Chem. Int. Ed. Engl.*, 2011, 50(41): 9697
151. X. Guo, C. Cui, M. Zhang, L. Huo, Y. Huang, J. Hou, and Y. Li, High efficiency polymer solar cells based on poly(3-hexylthiophene)/indene- C_{70} bisadduct with solvent additive, *Energy Environ. Sci.*, 2012, 5(7): 7943
152. Y. J. He, H. Y. Chen, J. H. Hou, and Y. F. Li, Indene- $C(60)$ bisadduct: a new acceptor for high-performance polymer solar cells, *J. Am. Chem. Soc.*, 2010, 132(4): 1377

153. Z. C. He, C. Zhang, X. F. Xu, L. J. Zhang, L. Huang, J. W. Chen, H. B. Wu, and Y. Cao, Largely enhanced efficiency with a PFN/Al bilayer cathode in high efficiency bulk heterojunction photovoltaic cells with a low bandgap polycarbazole donor, *Adv. Mater.*, 2011, 23(27): 3086
154. Y. Bai, J. Zhang, D. Zhou, Y. Wang, M. Zhang, and P. Wang, Engineering organic sensitizers for iodine-free dye-sensitized solar cells: red-shifted current response concomitant with attenuated charge recombination, *J. Am. Chem. Soc.*, 2011, 133(30): 11442
155. Z. Dong, X. Lai, J. E. Halpert, N. Yang, L. Yi, J. Zhai, D. Wang, Z. Tang, and L. Jiang, Accurate control of multishelled ZnO hollow microspheres for dye-sensitized solar cells with high efficiency, *Adv. Mater.*, 2012, 24(8): 1046
156. J. Zhang, J. Yu, M. Jaroniec, and J. R. Gong, Noble metal-free reduced graphene oxide-ZnxCd_{1-x}S nanocomposite with enhanced solar photocatalytic H₂-production performance, *Nano Lett.*, 2012, 12 (9): 4584
157. Q. Li, B. D. Guo, J. G. Yu, J. R. Ran, B. H. Zhang, H. J. Yan, and J. R. Gong, Highly efficient visible-light-driven photocatalytic hydrogen production of CdS-cluster-decorated graphene nanosheets, *J. Am. Chem. Soc.*, 2011, 133(28): 10878
158. S. Xin, Y. G. Guo, and L. J. Wan, Nanocarbon networks for advanced rechargeable lithium batteries, *Acc. Chem. Res.*, 2012, 45(10): 1759
159. Z. L. Gong, Y. X. Li, G. N. He, J. Li, and Y. Yang, Nanostructured Li₂FeSiO₄ electrode material synthesized through hydrothermal-assisted sol-gel process, *Electrochem. Solid-State Lett.*, 2008, 11(5): A60
160. F. F. Cao, Y. G. Guo, S. F. Zheng, X. L. Wu, L. Y. Jiang, R. R. Bi, L. J. Wan, and J. Maier, Symbiotic coaxial nanocables: Facile synthesis and an efficient and elegant morphological solution to the lithium storage problem, *Chem. Mater.*, 2010, 22(5): 1908
161. L. Huo, J. Hou, S. Zhang, H. Chen, and Y. Yang, A Polybenzo[1,2-*b*:4,5-*b'*]dithiophene derivative with deep HOMO level and its application in high-performance polymer solar cells, *Angew. Chem. Int. Ed.*, 2010, 49(8): 1500
162. D. J. Xue, S. Xin, Y. Yan, K. C. Jiang, Y. X. Yin, Y. G. Guo, and L. J. Wan, Improving the electrode performance of Ge through Ge@C core-shell nanoparticles and graphene networks, *J. Am. Chem. Soc.*, 2012, 134(5): 2512
163. Q. Zhang, Q. F. Dong, M. S. Zheng, and Z. W. Tian, Electrochemical energy storage device for electric vehicles, *J. Electrochem. Soc.*, 2011, 158(5): A443
164. L. Gu, C. Zhu, H. Li, Y. Yu, C. Li, S. Tsukimoto, J. Maier, and Y. Ikuhara, Direct observation of lithium staging in partially delithiated LiFePO₄ at atomic resolution, *J. Am. Chem. Soc.*, 2011, 133(13): 4661
165. D. W. Wang, F. Li, M. Liu, G. Q. Lu, and H. M. Cheng, 3D aperiodic hierarchical porous graphitic carbon material for high-rate electrochemical capacitive energy storage, *Angew. Chem. Int. Ed. Engl.*, 2008, 47(2): 373
166. X. F. Xie and L. Gao, Characterization of a manganese dioxide/carbon nanotube composite fabricated using an in situ coating method, *Carbon*, 2007, 45(12): 2365
167. J. J. Xu, K. Wang, S. Z. Zu, B. H. Han, and Z. X. Wei, Hierarchical Nanocomposites of Polyaniline Nanowire Arrays on Graphene Oxide Sheets with Synergistic Effect for Energy Storage, *ACS Nano*, 2010, 4(9): 5019
168. C. Chen, W. Ma, and J. Zhao, Semiconductor-mediated photodegradation of pollutants under visible-light irradiation, *Chem. Soc. Rev.*, 2010, 39(11): 4206
169. M. Zhang, Q. Wang, C. Chen, L. Zang, W. Ma, and J. Zhao, Oxygen atom transfer in the photocatalytic oxidation of alcohols by TiO₂: Oxygen isotope studies, *Angew. Chem. Int. Ed.*, 2009, 48(33): 6081
170. C. Y. Cao, J. Qu, W. S. Yan, J. F. Zhu, Z. Y. Wu, and W. G. Song, Low-cost synthesis of flowerlike -Fe₂O₃ nanostructures for heavy metal ion removal: Adsorption property and mechanism, *Langmuir*, 2012, 28(9): 4573
171. C. Y. Cao, P. Li, J. Qu, Z. F. Dou, W. S. Yan, J. F. Zhu, Z. Y. Wu, and W. G. Song, High adsorption capacity and the key role of carbonate groups for heavy metal ion removal by basic aluminum carbonate porous nanospheres, *J. Mater. Chem.*, 2012, 22(37): 19898
172. C. Y. Cao, J. Qu, F. Wei, H. Liu, and W. G. Song, Superb adsorption capacity and mechanism of flowerlike magnesium oxide nanostructures for lead and cadmium ions, *ACS Appl. Mater. Interfaces*, 2012, 4(8): 4283
173. W. Liu, F. Huang, Y. Liao, J. Zhang, G. Ren, Z. Zhuang, J. Zhen, Z. Lin, and C. Wang, Treatment of Cr^{VI}-containing Mg(OH)₂ nanowaste, *Angew. Chem. Int. Ed. Engl.*, 2008, 47(30): 5619
174. W. Liu, F. Huang, Y. Wang, T. Zou, J. Zheng, and Z. Lin, Recycling Mg(OH)₂ nanoadsorbent during treating the low concentration of CrVI, *Environ. Sci. Technol.*, 2011, 45(5): 1955
175. Q. Cao, F. Huang, Z. Zhuang, and Z. Lin, A study of the potential application of nano-Mg(OH)₂ in adsorbing low concentrations of uranyl tricarbonate from water, *Nanoscale*, 2012, 4(7): 2423
176. S. Guo and E. Wang, Noble metal nanomaterials: Controllable synthesis and application in fuel cells and analytical sensors, *Nano Today*, 2011, 6(3): 240
177. S. Guo and S. Dong, Biomolecule-nanoparticle hybrids for electrochemical biosensors, *Trends Analyt. Chem.*, 2009, 28(1): 96
178. D. Wen, S. Guo, J. Zhai, L. Deng, W. Ren, and S. Dong, Pt Nanoparticles Supported on TiO₂ Colloidal Spheres with Nanoporous Surface: Preparation and Use as an Enhancing Material for Biosensing Applications, *J. Phys. Chem. C*, 2009, 113(30): 13023
179. S. Guo and S. Dong, Graphene nanosheet: synthesis, molecular engineering, thin film, hybrids, and energy and analytical applications, *Chem. Soc. Rev.*, 2011, 40(5): 2644

180. M. Zhou, Y. Zhai, and S. Dong, Electrochemical sensing and biosensing platform based on chemically reduced graphene oxide, *Anal. Chem.*, 2009, 81(14): 5603
181. X. Wu, Y. Hu, J. Jin, N. Zhou, P. Wu, H. Zhang, and C. Cai, Electrochemical approach for detection of extracellular oxygen released from erythrocytes based on graphene film integrated with laccase and 2,2-azino-bis(3-ethylbenzothiazoline-6-sulfonic acid), *Anal. Chem.*, 2010, 82(9): 3588
182. K. Qian, J. Wan, L. Qiao, X. Huang, J. Tang, Y. Wang, J. Kong, P. Yang, C. Yu, and B. Liu, Macroporous materials as novel catalysts for efficient and controllable proteolysis, *Anal. Chem.*, 2009, 81(14): 5749
183. Y. Zhang, X. Wang, W. Shan, B. Wu, H. Fan, X. Yu, Y. Tang, and P. Yang, Enrichment of low-abundance peptides and proteins on zeolite nanocrystals for direct MALDI-TOF MS analysis, *Angew. Chem. Int. Ed. Engl.*, 2005, 44(4): 615
184. H. M. Xiong, X. Y. Guan, L. H. Jin, W. W. Shen, H. J. Lu, and Y. Y. Xia, Surfactant-free synthesis of SnO₂@PMMA and TiO₂@PMMA core-shell nanobeads designed for peptide/protein enrichment and MALDI-TOF MS analysis, *Angew. Chem. Int. Ed. Engl.*, 2008, 47(22): 4204
185. R. Tian, H. Zhang, M. Ye, X. Jiang, L. Hu, X. Li, X. Bao, and H. Zou, Selective extraction of peptides from human plasma by highly ordered mesoporous silica particles for peptide analysis, *Angew. Chem. Int. Ed. Engl.*, 2007, 46(6): 962
186. S. Song, Y. Qin, Y. He, Q. Huang, C. Fan, and H. Y. Chen, Functional nanoprobe for ultrasensitive detection of biomolecules, *Chem. Soc. Rev.*, 2010, 39(11): 4234
187. Y. M. Long, Q. L. Zhao, Z. L. Zhang, Z. Q. Tian, and D. W. Pang, Electrochemical methods-important means for fabrication of fluorescent nanoparticles, *Analyst*, 2012, 137(4): 805
188. D. Liu, W. Chen, K. Sun, K. Deng, W. Zhang, Z. Wang, and X. Jiang, Resettable, multi-readout logic gates based on controllably reversible aggregation of gold nanoparticles, *Angew. Chem. Int. Ed. Engl.*, 2011, 50(18): 4103
189. W. Qu, Y. Liu, D. Liu, Z. Wang, and X. Jiang, Copper-mediated amplification allows readout of immunoassays by the naked eye, *Angew. Chem. Int. Ed. Engl.*, 2011, 50(15): 3442
190. M. T. Zhu, G. J. Nie, H. Meng, T. Xia, A. Nel, and Y. L. Zhao, Physicochemical Properties Determine Nanomaterial Cellular Uptake, Transport, and Fate, *Acc. Chem. Res.*, 2013, 46(3): 622
191. B. Wang, X. He, Z. Y. Zhang, Y. L. Zhao, and W. Y. Feng, Metabolism of nanomaterials in vivo: Blood circulation and organ clearance, *Acc. Chem. Res.*, 2013, 46(3): 761
192. Y. Liu, Y. L. Zhao, B. Y. Sun, and C. Y. Chen, Understanding the toxicity of carbon nanotubes, *Acc. Chem. Res.*, 2013, 46(3): 702
193. Y. L. Zhao, G. M. Xing, and Z. F. Chai, Nanotoxicology: Are carbon nanotubes safe? *Nat. Nanotech.*, 2008, 3: 191
194. H. Yang, C. J. Sun, Z. L. Fan, X. Tian, L. Yan, L. B. Du, Y. Liu, C. Y. Chen, X. J. Liang, G. J. Anderson, J. A. Keelan, Y. L. Zhao, and G. J. Nie, Effects of gestational age and surface modification on materno-fetal transfer of nanoparticles in murine pregnancy, *Scientific Reports*, 2012, 2(847): 1
195. C. C. Ge, J. F. Du, L. N. Zhao, L. Wang, Y. Liu, D. Li, Y. Yang, R. H. Zhou, Y. L. Zhao, Z. F. Chai, and C. Y. Chen, Binding of blood proteins to carbon nanotubes reduces cytotoxicity, *Proc. Natl. Acad. Sci. USA*, 2011, 108: 16968
196. S. G. Kang, G. Q. Zhou, P. Yang, Y. Liu, B. Y. Sun, T. Huynh, H. Meng, L. N. Zhao, G. M. Xing, C. Y. Chen, Y. L. Zhao, and R. H. Zhou, Molecular mechanism of pancreatic tumor metastasis inhibition by Gd@C82(OH)₂₂ and its implication for de novo design of nanomedicine, *Proc. Natl. Acad. Sci. USA*, 2012, 109(38): 15431
197. Y. Y. Li, Y. L. Zhou, H. Y. Wang, S. Perrett, Y. L. Zhao, Z. Y. Tang, and G. J. Nie, Chirality of glutathione surface coating affects the cytotoxicity of quantum dots, *Angew. Chem. Int. Ed.*, 2011, 50: 5860
198. C. Sun, H. Yang, Y. Yuan, X. Tian, L. Wang, Y. Guo, L. Xu, J. Lei, N. Gao, G. J. Anderson, X. J. Liang, C. Chen, Y. Zhao, and G. Nie, Controlling assembly of paired gold clusters within apoferritin nanoreactor for in vivo kidney targeting and biomedical imaging, *J. Am. Chem. Soc.*, 2011, 133(22): 8617
199. C. C. Ge, F. Lao, W. Li, Y. Li, C. C. Chen, Y. Qiu, X. Mao, B. Li, Z. F. Chai, and Y. L. Zhao, Quantitative analysis of metal impurities in carbon nanotubes: Efficacy of different pretreatment protocols for ICPMS spectroscopy, *Anal. Chem.*, 2008, 80(24): 9426
200. Y. Qu, W. Li, Y. Zhou, X. Liu, L. Zhang, L. Wang, Y. F. Li, A. Iida, Z. Tang, Y. Zhao, Z. Chai, and C. Chen, Full assessment of fate and physiological behavior of quantum dots utilizing *Caenorhabditis elegans* as a model organism, *Nano Lett.*, 2011, 11(8): 3174
201. X. He, Z. Y. Zhang, J. S. Liu, Y. H. Ma, P. Zhang, Y. Y. Li, Z. Q. Wu, Y. L. Zhao, and Z. F. Chai, Quantifying the biodistribution of nanoparticles, *Nat. Nanotechnol.*, 2011, 6(12): 755